REVIEW

Check for updates

Unveiling the potential of Ti₃C₂Tₓ MXene for gas sensing: recent developments and future perspectives

Nitesh K. Chourasia, [a] Ankita Rawat,[a] Ritesh Kumar Chourasia,[b] Hemant Singh,[a] Ramesh Kumar Kulriya,[c] Vinod Singh [c] and Pawan Kumar Kulriya *[a]

Ti₃C₂Tₓ MXene, a two-dimensional transition metal carbide, has garnered significant attention as a promising material for gas sensing applications due to its exceptional properties. In this comprehensive review article, we provide an in-depth overview of the recent advancements in the field of Ti₃C₂Tₓ-based gas sensors. We summarize the various synthesis methods employed for Ti₃C₂Tₓ MXene production, including selective etching of MAX phase precursor materials and controlled annealing processes to customize its surface chemistry and properties. We thoroughly review the gas sensing properties of Ti₃C₂Tₓ MXene towards a wide range of gases, including volatile organic compounds (VOCs), toxic gases, and other target gases. We provide detailed insights into the gas sensing performance of Ti₃C₂Tₓ-based gas sensors, including sensitivity, selectivity, response and recovery times, and stability, under various temperature and gas concentration conditions. The gas sensing mechanisms involving charge transfer and surface chemisorption processes between gas molecules and the Ti₃C₂Tₓ MXene surface are also discussed based on experimental and theoretical studies. Furthermore, we highlight the strategies employed to enhance the gas sensing performance of Ti₃C₂Tₓ-based gas sensors, such as surface functionalization, doping, and hybridization with other materials. We discuss the influence of various factors, such as annealing temperature, surface modification, and device configurations, on the gas sensing properties of Ti₃C₂Tₓ MXene-based gas sensors. Finally, we address the challenges and future perspectives of Ti₃C₂Tₓ-based gas sensors, in25cluding the need for standardized testing protocols, long-term stability, and scalability of fabrication processes. Our comprehensive review aims to inspire further research efforts and promote the development of Ti₃C₂Tₓ MXene-based gas sensors with enhanced performance and broader applications, highlighting the promising potential of Ti₃C₂Tₓ MXene as a cutting-edge material for gas sensing applications.

[a] School of Physical Sciences, Jawaharlal Nehru University, New Delhi-110067, India. E-mail: pkkulriya@mail.jnu.ac.in

[b] Department of Physics, Samastipur College, (A Constituent College of L.N.M.U. Darbhanga-846004), Samastipur-848134, India

[c] Department of Applied Physics, Delhi Technological University, New Delhi-110042, India

1. Introduction

In our contemporary world, marked by swift industrial growth and urban development, the significance of sensors capable of precisely identifying a wide range of hazardous gases has grown considerably. Consequently, sensitive materials, serving as pivotal elements in gas sensor technology, have garnered significant attention in ongoing research endeavors. This heightened focus is driven by their crucial roles in enhancing industrial safety, safeguarding the environment, and preserving personal well-being.[1,2] At present, several materials have been investigated and established for gas sensors, such as metal oxides (MO), carbon-based materials, metal–organic frameworks (MOF), conductive polymers, rare-earth oxides, *etc.*[3–12] Metal oxide semiconductor (MOS) can be classified into two types, n-type (*e.g.*, ZnO, SnO₂, TiO₂, *etc.*) and p-type (*e.g.*, SnO, CuO, WO₃, *etc.*). MO is the preferred choice for researchers as a transistor, photodetector, and gas sensor owing to its high sensitivity, high electron mobility, good transparency, low off-state current, chemical stability, compact dimensions, facile fabrication, and affordability.[13–24] For instance, Saini *et al.* used nanowires of Zn(ɪɪ) 2,3,9,10,16,17,23,24-octakis(octyloxy)-29*H*,31*H*-phthalocyanine (ZnPcOC₈) and nanoflowers of Cu(ɪɪ) 2,3,9,10,16,17,23,24-octakis(octyloxy)-29*H*,31*H*-phthalocyanine (CuPcOC₈) for a Cl₂ sensor at room temperature.[25] The fabricated sensor has a detection limit as low as 5 ppb and with responses as high as 715% and 550% within 10 s and 15 s by

using simple and cost-effective self-assembly techniques. Chaloeipote et al. employed 3D printing technology for the synthesis of CuO, and the resulting CuO sensor demonstrated a favorable response to the detection of NO_2, registering a response of 14.17% when detecting 200 ppm NO_2 at room temperature. Nonetheless, conventional gas sensors constructed with MO as gas-sensitive materials often attain higher response levels within the temperature range of 200 °C to 500 °C.[26] This requirement for elevated temperatures not only escalates the cost of gas detection but also introduces potential safety hazards due to the elevated operating temperatures. Wang et al. employed KIT-6 as the rigid template for the synthesis of WO_3 with incorporated Au particles. The resulting Au–WO_3 sensor exhibited remarkable sensitivity in detecting trimethylamine, with a rapid response time of just

Nitesh K. Chourasia

Dr Nitesh K. Chourasia is working as a National Postdoctoral Fellow at the School of Physical Sciences, Jawaharlal Nehru University (JNU), New Delhi, India. He has obtained his MSc degree from Banaras Hindu University (BHU), and his PhD degree from the School of Materials Science and Technology, Indian Institute of Technology, Banaras Hindu University (IIT-BHU), Varanasi, India. His research interest mainly focuses on new types of ion-conducting dielectrics for electronic and optoelectronic devices (e.g. transistors, photodetectors, sensors, etc.). His current research activities are to synthesize $Ti_3C_2T_x$ MXene for toxic gas sensors.

Ankita Rawat

Ankita Rawat is a PhD student at the School of Physical Sciences, Jawaharlal Nehru University (JNU), New Delhi, India. She has completed her MSc from the Department of Physics, IIT Delhi. Her research interest is mainly focused on 2D materials-based electronic and optoelectronics devices (e.g. transistors and photodetectors). She is also working on $Ti_3C_2T_x$ MXene-based gas sensors.

Ritesh Kumar Chourasia

Dr Ritesh Kumar Chourasia earned his Master's in Physics (Specialization-Electronics) and PhD from the Institute of Science, Banaras Hindu University (Varanasi, India). He has qualified for the highly competitive exam CSIR-JRF (junior research fellow) in Physical Sciences for getting a PhD fellowship and eligibility required for a permanent faculty position in India. He has also qualified for UGC-NET in Electronic Sciences, an international examination GATE-Physics, and JEST-Physics. He joined as an Assistant Professor at Lalit Narayan Mithila University, Darbhanga, in 2017. His current research interest is theoretical modeling including DFT studies of some novel materials, simulation, and device fabrication in the photonics and photovoltaics field. He has published 24 research papers in international journals of repute, 2 patents, and 8 book chapters.

Pawan Kumar Kulriya

Pawan Kumar Kulriya is working as an Associate Professor of Physics at the School of Physical Sciences at the Jawaharlal Nehru University (JNU) New Delhi. Before joining JNU, he was also associated as a Scientist-F in the Materials Science Group, Inter-University Accelerator Centre (IUAC) New Delhi, India for 17 years. He holds both a PhD in Physics and an MTech in Solid State Materials from the Indian Institute of Technology (IIT) Delhi and an MSc in Physics from the University of Rajasthan, Jaipur. He was awarded a prestigious Fulbright-Nehru Postdoctoral Fellowship by the U.S. Department of State at the Rensselaer Polytechnic Institute in New York, USA where he has carried out a research project on the materials for the immobilization of high level radioactive waste. Dr Kulriya has more than 140 peer-reviewed papers in leading international journals. His research on Experimental Condensed Matter Physics includes nano-materials for nuclear energy systems, materials for radiation shielding, development of advanced ceramic and high entropy alloys as well as their performance evaluation under the extreme environment of high temperature and radiation. Apart from this, he is currently working on 2D materials for gas sensing applications.

1 second and a response rate of 42.56% when exposed to 100 ppm trimethylamine at 268 °C.[27] Sun *et al.* reported H_2 gas sensor using ZnO nanofiber film (average diameter of ∼60 nm). Within the temperature range of 210–330 °C, upon exposure to 20 ppm H_2 gas, the resistance of the ZnO nanofiber film increased, and the sensitivity ∼28.84% at 270 °C.[28] Kumar *et al.* reported room temperature chemiresistive sensors using hexadecafluorinated copper phthalocyanine (F16CuPc) and graphene oxide (rGO) hybrid materials. The fabricated sensor is highly sensitive to Cl_2 gas with a detection limit up to ppb level.[29] Generally, gas sensors utilizing MOSs typically demand elevated operating temperatures to attain their peak gas-sensing capabilities. This not only results in heightened energy consumption but also raises the potential danger of explosions when detecting flammable and explosive gases. Moreover, the requirement for high operating temperatures restricts their suitability for use in wearable gas sensors. Hence, there is a need to innovate and create new materials for gas sensing that can operate at ambient room temperature.

Recently, two-dimensional (2D) materials have attracted much attention to research society in different scientific applications. Since the discovery of $Ti_3C_2T_x$ MXene in 2011, 2D transition metal carbides/nitrides (together referred to as MXenes) have involved significant research consideration.[30,31] Owing to their outstanding mechanical, biological and electrical properties such as efficient electromagnetic interference (EMI) shielding, large surface-to-volume ratio, extraordinary electrical conductivity, water dispersibility, high energy capacity, and excellent antibacterial activity, this newly discovered category of materials are important in a wide range of different areas of research.[32–37] In the case of sensors, the replacement of traditional sensor materials (*e.g.*, metal alloys and carbon) has been crucial in light of the fact that unadventurous technology is progressively reaching its limits in terms of potential improvements to sensor performance. As a result, significant exertions have been made to investigate the use of MXenes in a variety of sensor technologies for biological, chemical, mechanical, optical, and gas sensors.[38–42] MXene's 2D structure, having diverse terminal functionalization groups, provides a large number of active surface sites that can help as quick-to-respond sensor platforms for numerous exterior boosts. Apart from this, the high electrical conductivity of MXene is advantageous to attaining low noise.[43] Because of these unique characteristics, MXenes appear to be a promising alternative sensor material that can provide high sensitivity, extraordinarily low-level detectivity (ppb level), high selectivity, and low power consumption as well as can operate at ambient conditions. Last but not least, the fact that MXenes are easily dispersed in water enables environmentally responsible manufacture as well as amendment treatments, which further increases their utility in the processing industry. $M_{n+1}X_nT_X$ is the general formula of MXenes, where n demonstrates structures. The structure of MXene is known to be influenced by its MAX ($M_{n+1}X_nT_X$) phase precursor, which has previously constrained the MXene family to materials containing 2, 3, or 4 atomic layers of transition metals.[44,45] Recently introducing a new MXene variant, M_5X_4, which contains five atomic layers of transition metals.[46] M represents an early

transition metal (*e.g.*, Ti, Mo, and V), and X refers to carbon/nitrogen or their mixture. At the same time, T_x stands for numerous surface terminations, *e.g.*, oxygen (=O), hydroxyl (–OH), and fluorine (–F).[47] MXene research has sparked interest due to its superior features and ease of processing; hence till now over 30 compositions of MXene have already been reported.[48,49] Furthermore, the remarkable electrical properties and elevated electron density at the Fermi level exhibited by $Ti_3C_2T_x$ make it highly amenable to surface modification through the introduction of specific terminating species. As a consequence, these distinctive characteristics of $Ti_3C_2T_x$ MXene make it particularly promising for sensitive interactions with toxic gas molecules, rendering it a viable candidate for gas-sensing applications. One effective approach involves the integration of $Ti_3C_2T_x$ nanomaterials with other substances, such as transition metal dichalcogenides (TMDs), metal oxide semiconductors (MOS), and graphene, resulting in potential hybrid materials well-suited for gas sensing applications.[50] In brief, $Ti_3C_2T_x$ MXene materials have emerged as a promising advancement in the realm of gas sensors, offering numerous advantages over conventional metal oxides. Notably, $Ti_3C_2T_x$ MXenes display highest sensitivity to various gases, enabling the detection of even trace concentrations with greater accuracy. Moreover, $Ti_3C_2T_x$ MXene-based sensors exhibit faster response times, crucial for rapid gas detection in safety-critical applications. Unlike many metal oxide sensors that require elevated operating temperatures, $Ti_3C_2T_x$ MXenes can function effectively at room temperature, reducing energy consumption and eliminating the safety risks associated with high temperatures. Their superior selectivity, durability, and flexibility, along with the ability to engineer their properties, make $Ti_3C_2T_x$ MXene materials a compelling choice for gas sensors, especially in applications demanding precision, reliability, and versatility.

Herein, we systematically review the synthesis process, physical properties, and sensing applications in different areas of $Ti_3C_2T_x$ MXenes. Fig. 1 shows the structure of this review article. At first, we will start with the synthesis of MXenes using different approaches (*e.g.* top down and bottom up approach), further our focus will be the properties of MXenes that will be useful of sensing applications. At last, this review article emphasizes the different types of $Ti_3C_2T_x$ MXenes (*e.g.* pristine, functionalized and composite) for gas sensing applications. Although we will discuss different types of possible MXenes but our goal is to cover the state-of-the-art research accomplishments of using $Ti_3C_2T_x$ MXene and their application in gas sensors, including novel device architecture fundamental sensing mechanisms, and offer wise prospects for upcoming endeavours. This review article offers a fresh perspective on the utilization of $Ti_3C_2T_x$ MXene in gas sensing, surpassing earlier review articles in terms of its comprehensive coverage of recent developments and its forward-looking insights. Unlike previous reviews, this article provides a more up-to-date and detailed examination of the latest advancements in MXene-based gas sensors. It highlights the cutting-edge techniques and applications that have emerged, shedding light on how
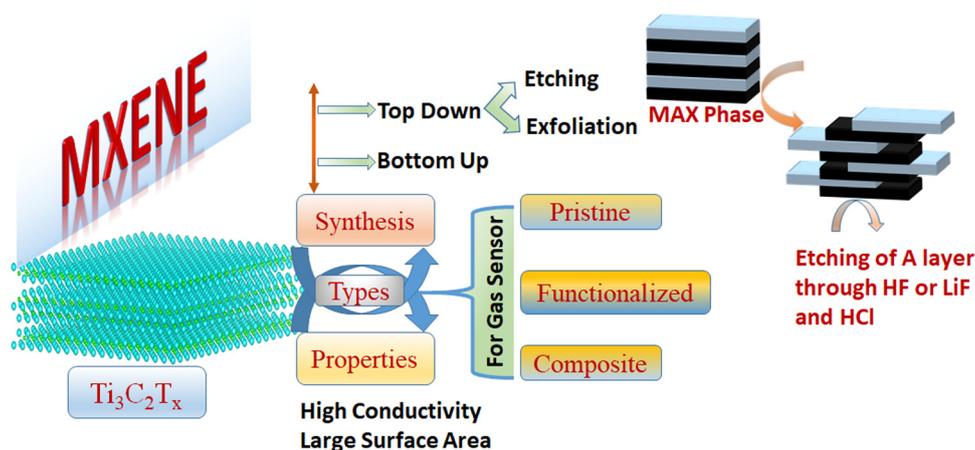
Fig. 1 Structure of the review article.

$Ti_3C_2T_x$ MXene materials can be tailored for enhanced gas-sensing performance. This review articles also summarize theoretical studies of MXene-based gas sensors using Density Functional Theory (DFT) and Molecular Dynamics (MD) simulations, which provide insights into the adsorption mechanisms and dynamic behavior of gas molecules on MXene surfaces, allowing for a comprehensive understanding of sensor performance, selectivity, and stability at the atomic level. By offering future perspectives, it goes beyond summarizing existing knowledge and sets a forward-looking agenda for researchers and engineers, helping to shape the future of $Ti_3C_2T_x$ MXene-based gas sensing technology. This focus on recent developments and future directions positions the article as a valuable resource in the field of gas sensing, providing a more current and forward-thinking perspective compared to earlier review articles.
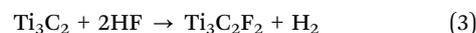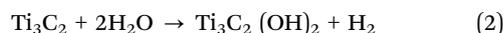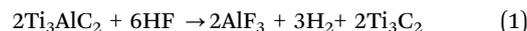
2. Technique for synthesis of MXenes

The techniques used to synthesize the MXene significantly affect its structure and surface functional groups, which in turn impacts the sensor's performance. The top-down etching from MAX phases is now the most widely utilized method for making MXene nanosheets. The layered structure of the MAX phase is made up of densely packed M layers and X atoms that occupy the octahedral sites and are bonded together with A atoms. In general, the M–A bond is typically thought of as a metallic bond, while the M–X bond can exhibit ionic, metallic, or covalent properties.[51] There are mainly two steps involved in the synthesis of MXene, i.e., (1) selective etching of A layer from MAX phase and (2) delamination of MXenes from MAX phase;[52] both steps will discuss one by one.

2.1 Top-down approach

2.1.1 Etching. In the very first synthesis of MXene, it was suggested that an aqueous solution of hydrofluoric acid (HF) could etch the MAX phase of Ti_3AlC_2, and $Ti_3C_2T_x$-based MXene can be formed after selective removal of the Al layer. This

synthesis method is known as top-down synthesis and is also referred to as the main synthesis route nowadays. The etching of Ti_3AlC_2 involves three reaction steps, as mentioned below

$$2Ti_3AlC_2 + 6HF \rightarrow 2AlF_3 + 3H_2 + 2Ti_3C_2 \quad (1)$$

$$Ti_3C_2 + 2H_2O \rightarrow Ti_3C_2(OH)_2 + H_2 \quad (2)$$

$$Ti_3C_2 + 2HF \rightarrow Ti_3C_2F_2 + H_2 \quad (3)$$

As one can see from eqn (1), during etching, AlF_3 will be a byproduct that is water-insoluble; it's vital to pick the right temperature and time to avoid precipitation of AlF_3. For chemical etching, one needs to consider different reaction parameters like HF concentration, reaction time, optimum temperature, etc. According to the literature, $M_{n+1}AX_n$, with a large n number, necessitates a long etching time, a low pH value, and high etching temperature.[53] Therefore, a high concentration of HF is always beneficial for preferential etching of the Al layer, which can be confirmed from the structural investigation. XRD pattern exhibits a clear downshift of the (002) peak and displays the successful Al etching in Ti_3AlC_2.[54] Furthermore, the experimental results showed that the HF concentration can be used to rectify vacancy defects caused by the removal of surface Ti atoms.

As we know that handling HF is quite difficult, and apart from that, HF is highly corrosive in nature and not environment friendly. Furthermore, HF has a proclivity for over-corroding, resulting in defects in MXene. In 2014, NH_4HF_2 was used as an etchant to avoid using toxic HF directly.[55] This is a significantly safer and milder alternative. In the same year, researchers also utilized LiF and HCl mixture for the etching of the Al layer in Ti_3AlC_2 to form $Ti_3C_2T_x$.[56] The reaction time was 45 hours at a constant temperature of 40 °C, and the results showed that the presence of protons and fluorine ions is essential for effective etching. Later on, researchers also put more effort into refining this method by varying the feeding ratio of LiF and MAX (LiF : MAX = 5 : 1 or 7.5 : 1).[57] Excess LiF was found to promote Al etching and Li^+ intercalation, resulting in $Ti_3C_2T_x$ MXene

nanosheets with identical thickness, larger size, and fewer defects. In most cases, the etching process transforms solid dense MAX into structures resembling accordions with loosely collected layers, and these formations are also referred to as multilayer MXenes. As a result, an exfoliation step is compulsory for multi-layer MXenes into monolayers.

2.1.2 Exfoliation. Etching and delamination are the two primary processes that make up the majority of the MXene exfoliation process from the MAX phase. In the first step, a chemical etching process is used to remove the "A" layer from the middle of the MAX layers. Each MXene layer must be delaminated from the etched MAX phase in the second step. This procedure for the synthesis of MXene was carried out in a number of different ways, as shown in Fig. 2.[58] Each technique either incorporates HF into the MAX solution directly or introduces it indirectly through the use of LiF. The chemical connection that holds the M and X layers together can be broken apart if they are subjected to sonication, intercalants like dimethyl sulfoxide (DMSO), or ionic solutions. In any of these three scenarios, the layers are more likely to delaminate. Apart from this, LiF and HF are also favorable for non-Ti-based MXene (*e.g.*, niobium (Nb), vanadium (V), *etc.*)[59,60]

The nanosheets of MXene were able to be exfoliated into a single layer by first inserting large organic molecules into the interlayers of the accordion-like structure and then subjecting the structure to ultrasonication or mechanical vibration.[52] This allowed the nanosheets to be rearranged into a single layer. The frequently used intercalants comprise NH_4^+, dimethyl sulfoxide, hydrazine, urea, and tetrabutylammonium hydroxide (TBAOH).[61–63] Recently, Chia *et al.* reported that by using TBAOH as the intercalant, one could exfoliate $Ti_3C_2T_x$ MXene from HF etching products.[64] After removing the A layer, expanding MAX powder that contained micron-sized flakes led to the formation of Ti_3C_2–HF, which was then delaminated into MXenes with one or more than one layers by reducing the strength of the interlayer contact with TBAOH.

2.2 Bottom-up approach

In addition to the top-down tactics that were discussed above, a multifunctional bottom-up approach known as chemical vapor deposition (CVD) was developed for the purpose of synthesizing high-quality and large-area MXenes. In contrast to the top-down method, which has a complex combination of groups and low controllability, the bottom-up approach has the advantage of accurately manipulating the morphology and termination groups of MXenes. The synthesis process is crucial for under-standing the inherent characteristics of MXenes. Researchers reported ultrathin Mo_2C, WC, and TaC MXene crystals on Cu/Mo foil using CVD, and all of them have fewer defects with larger lateral dimensions.[65] The bottom-up synthesis technique of MXenes is still a big problem due to the costly equipment and tedious procedures.

In addition, if the MXene was subjected to mechanical vibration or sonication, it would contract and develop further defects. The inherent properties of 2D TMCs and TMNs have been hindered due to the chemical modification and mechan-ical damage that has been done to MXenes. The constituent parts of the mother 3D MAX phase have a direct influence on the structure and species of MXenes and *vice versa*. All of the MXenes that have been synthesized up to this point contain structures of the M_2X, M_3X_2, and M_4X_3 types. New synthesis methods are urgently required to improve the quality of 2D TMCs and TMNs as well as to expand the family of these materials because these MX-structured materials make up a large class of TMCs and TMNs and have a variety of fascinating properties.

The CVD production of high-quality ultrathin TMCs crystals utilizing a bilayer metal foil as a growth substrate was initially reported in 2015 by Xu *et al.*, who was also the first to reveal the technique.[65] The stack of Cu/Mo foils was annealed in hydro-gen (H_2) to a temperature that was higher than 1085 °C, which is the melting point of copper. Following this step, methane was injected, which led to the formation of Mo_2C crystals on the
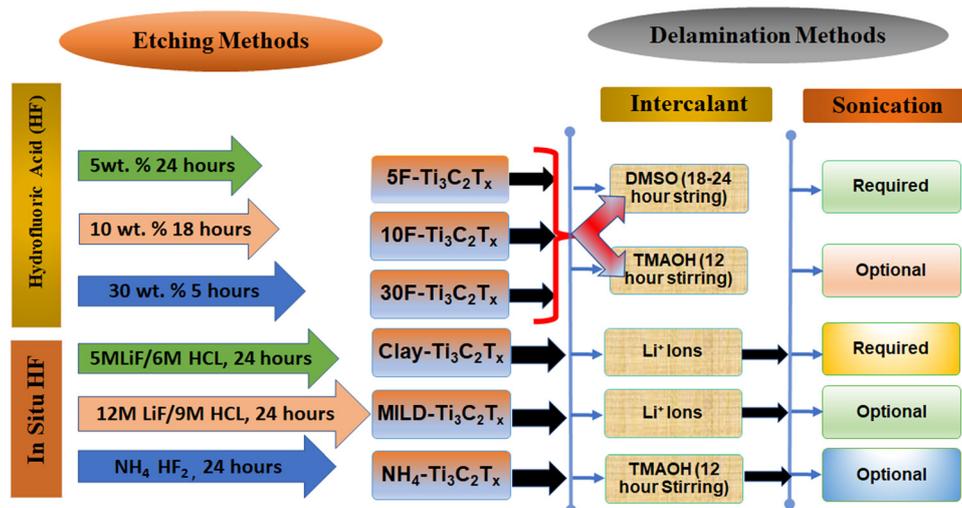

Fig. 2 Schematic diagram of the synthesis route of $Ti_3C_2T_x$ MXene. Reproduced with permission from ref. 58 Copyright 2020. MDPI (open Access).

surface of the liquid copper. During the course of development, the top layer of liquid Cu plays several crucial tasks that are essential to the process. Meanwhile, it participates in the process of converting methane into carbon atoms by acting as a catalyst, and it serves as a pathway for controlling the diffusion of molecular molybdenum from the molybdenum foil to the surface of the liquid copper. On the surface of the liquid Cu, ultrathin Mo_2C crystals form due to a process involving carbon and molybdenum atoms. In addition, due to the significant differences in the chemical reactivity of copper and molybdenum carbide (Mo_2C), copper acts as a sacrificial layer after Mo_2C is developed. This allows the transfer of Mo_2C to desired target substrate through etching. A bottom-up method, such as CVD, can produce high-quality films on various substrates; however, this method is not typically utilized in the production of MXenes because the films produced using this method are not mono-layers but relatively thinner films. The CVD was the method Xu and colleagues used to fabricate thin films of Mo_2C, WC, and TaC, for example.[66] In spite of this, even the most imperceptibly thin Mo_2C films consisted of at least six layers of Mo_2C, as opposed to a single layer of MXenes. To synthesize ultrathin TaN, Wang *et al.* used NH_3 as a nitrogen source and Cu/Ta foil as a growth substrate at 1077 °C. Copper foil maintains a solid state throughout CVD development. According to the images obtained from the TEM, both TaN crystals are single crystals. In addition, ultrathin TaB crystals were produced by employing boron powder as the source of element Wang *et al.* synthesised zirconium based MXenes (*e.g.* Zr_2CCl_2 and Zr_2CBr_2) by utilizing direct CVD techniques.[67] These two zirconium MXenes seemed in the same common morphology as that of the Ti–MXenes. In summary, the choice between bottom-up and top-down synthesis methods for MXene can influence its gas sensing properties. Bottom-up synthesis offers precise control over composition and structure, while top-down synthesis provides scalability but may yield less controlled surfaces. Both approaches have their advantages and considerations depending on the specific gas sensing requirements and desired performance characteristics.

3. Properties of MXene

High electrical conductivity, unique layered structure, wide specific surface area, and excellent dispersity distinguish MXenes from other functional materials, paving the way for further research and development in the sensor industry.[68] In addition to its superior conductivity, the most well-liked $Ti_3C_2T_x$ MXene also has a large surface area and an abundance of surface functional groups.[69]

3.1 Stability

The key parameter which decides the stability of MXene is; reaction conditions, solutions, and composition. Since, $Ti_3C_2T_x$ MXene is easily oxidized in the water and air, its environmental stability is an important study topic, as is its stability and service life during the sensor fabrication and utilization.

Because the oxidation of MXene often begins at the edge of the molecule and then spreads throughout the molecule, it is impossible for the entire molecule to be oxidized at the same time. Oxidation proceeds most slowly in the solid state and most quickly in the liquid state. The reaction of oxidation can be understood from the below reaction

$$Ti_3C_2O_2 + 4H_2O \rightarrow 3TiO_2 + 2C + 4H_2$$

MXene's fragile oxidation resistance is one of the challenges it faces in the process of usage, and it's worth looking into ways to alleviate the performance loss affected by oxidation. $Ti_3C_2T_x$ MXene can be effortlessly transformed into TiO_2 through annealing at either 1150 °C for thirty seconds or 400 °C for a longer time.[70,71] Some of MXene's benefits, like conductivity and capacitance, are often sacrificed during oxidation. As reported earlier, the ionic group of polyphenylene has the ability to effectively occupy the edge of the MXene sheet, which protects it from being oxidized by the water molecules.[72]

3.2 Electrical properties

The electrical properties of a single layer of $Ti_3C_2T_x$ MXene are worth researching in order to better understand its electrical performance and potential application in sensors. The band gap in MXene arises due to surface functionalization; otherwise, all MXenes exhibit metallic behaviour. The metallic $Ti_3C_2T_x$ material really does have the capacity to serve as an electrode for super capacitors. The performance of electrochemical capacitor devices is significantly influenced by the electronic conductivity of MXene. After being functionalized, some MXenes transform into semiconductors with energy gaps ranging from 0.25 to 2.0 eV.[73]

3.3 Mechanical properties

Because of their exceptional in-plane tensile characteristics, bending tolerance, and flexibility, MXenes are perfect for use in the fabrication of bendable electrodes and other electrical devices.[56] The surface terminations of MXenes have a significant impact on the mechanical characteristics. MXenes with an O termination are expected to have extremely high stiffness; however those with F and OH terminations exhibit lower elastic stiffness than O-terminated MXenes. That is why bonding strength between Ti–O being stronger than in the situations of Ti–OH and Ti–F. The flexibility of the surface-functionalized MXenes is greater than that of bare MXenes. The $Ti_3C_2T_x$ materials also have a remarkable degree of flexibility and tensile resistance. The 5 μm thick $Ti_3C_2T_x$ sheet can tolerate 1.3 MPa or roughly 4000 times of own weight, with no any observable distortion or fracture.[74]

4. Important characteristics of gas sensors

The main characteristic of a gas sensor is determined by a few critical parameters such as sensitivity, selectivity, stability, resolution, and response/retrace time shown in Fig. 3.
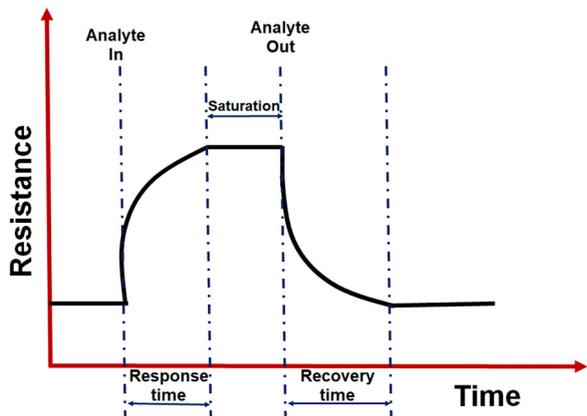
Fig. 3 Important characteristics of a typical metal oxide-based gas sensor.

• Sensitivity or response: it is defined as a relative change in sensor signal per unit concentration of the given analyte. Sensitivity (S) is often expressed as R_a/R_g for reducing gases or R_g/R_a for oxidizing gases, where R_a denotes the resistance of the gas sensors in the reference gas (typically air) and R_g denotes the resistance in the reference gas containing the target gases.

• Selectivity: the ability to selectively identify the particular analyte in the presence of other analytes.

• Stability: the time period over which the sensor retains its original characteristics.

• Detection limit: the lowermost concentration difference can be eminent by the sensors.

• Response time and recovery time: the response and recovery time was defined as the time required for 90% of the total resistance change to occur while introducing and removing the analyte.

4.1 Working principle and mechanism of chemiresistive gas sensor

A chemiresistive gas sensor is a remarkable device designed to detect the presence of specific gases by measuring changes in the electrical resistance or conductivity of a sensing material when it interacts with the target gas. The best example of chemiresistive gas sensor are metal oxide (MO) gas sensor. The heart of any chemiresistive gas sensor is the sensing material. The choice of sensing material is pivotal to the sensor's performance because different materials exhibit varying levels of sensitivity to different gases. Common sensing materials include metal oxides, conducting polymers, and organic materials, each with its unique gas-sensing mechanisms. The gas sensing mechanism of a chemiresistive gas sensor primarily involves two fundamental processes: adsorption and chemisorption.

4.1.1 Absorption mechanism. Adsorption is the process by which gas molecules adhere to the surface of the sensing material without forming strong chemical bonds. It occurs due to weak van der Waals forces, electrostatic interactions, or physisorption. When a gas molecule interacts with the surface of the sensing material, it may physically adsorb onto the surface or get trapped in surface defects or pores. This adsorption process can lead to a change in the electronic structure of the sensing material. In the case of semiconducting materials like MOs or carbon nanotubes, gas adsorption can alter the concentration of charge carriers (electrons or holes) in the material's crystal lattice.

4.1.2 Chemisorption mechanism. Chemisorption is a more specific and stronger form of gas–surface interaction than adsorption. It involves the formation of chemical bonds between gas molecules and surface atoms of the sensor material. In chemisorption, the gas molecules undergo a chemical reaction with the surface atoms, resulting in the creation of new chemical entities on the sensor's surface. The formation of these chemical bonds can lead to significant changes in the electronic structure of the sensing material, including changes in the number of charge carriers and their energy levels. The strength of chemisorption depends on the nature of the gas and the surface chemistry of the sensing material. Some gases chemisorb readily, while others may only adsorb weakly or not at all.

4.2 Factors affecting gas sensing performance

Several factors can influence the gas sensing mechanism and the performance of sensor:

1. Sensing material: the choice of sensing material is crucial and depends on the target gas or gases. Different materials have varying degrees of sensitivity to specific gases.

2. Target gas: the type of gas to be detected plays a significant role. Different gases have distinct chemical properties, and their interactions with the sensing material vary accordingly.

3. Temperature: temperature can influence the gas-sensing mechanism by altering the kinetics of adsorption and desorption processes. Many chemiresistive sensors operate at elevated temperatures to enhance sensitivity.

4. Humidity: humidity levels can affect the adsorption and chemisorption processes. Some sensors are sensitive to changes in humidity, which can lead to false readings.

5. Interfering gases: the presence of other gases in the environment can interfere with the sensor's response to the target gas. Selectivity is a critical consideration in sensor design.

In conclusion, chemiresistive gas sensors operate on the fundamental principles of adsorption and chemisorption. These mechanisms lead to changes in the electrical conductivity or resistance of a sensing material when it interacts with a specific target gas. The choice of sensing material, target gas, environmental conditions, and the presence of interfering gases all influence the sensor's performance. Understanding the gas sensing mechanism is essential for designing and optimizing chemiresistive gas sensors for various applications.

4.3 Sensing mechanism of $Ti_3C_2T_x$ MXene based gas sensor

The gas-sensing mechanisms in typical MO gas sensors are closely tied to the exchange of electrons, which occurs as a result of electron donation or acceptance from the target gas. Nevertheless, the gas-sensing mechanisms of MXenes exhibit

greater complexity compared to the conventional charge-transfer model. In the previous report on $Ti_3C_2T_x$ MXene based gas sensor, p-type sensing behavior was observed for ethanol, methanol, acetone, and ammonia gas at room temperature.[75] However, in subsequent investigations, it was observed that $Ti_3C_2T_x$ MXene consistently exhibited an increase in resistance when exposed to either oxidizing or reducing gases.[74,76] Based on the above observations, researchers proposed two possible mechanism. (1) MXene exhibits metallic characteristics rather than semiconductor behavior, and the adsorption of gas can diminish the number of carriers while raising the channel resistance of MXene,[77] and (2) the expansion of MXene inter-layers upon exposure to gases obstructs its electron transport in the out-of-plane direction.[78] Both of these mechanisms can clarify why MXenes consistently display a positive response to all gases. Though, according to Yang *et al.* report, the response signal of $Ti_3C_2T_x$ MXene had a shift from positive to negative followed by NaOH treatment.[79] The change in response direction is ascribed to the rise in the O/F ratio, suggesting that surface terminations also play a noteworthy role in gas-sensing behavior. However, the fundamental mechanism behind this transformation remains unclear.

In sensors, employing hybrid structures combining MXenes and other materials, the sensor's response direction frequently hinges on the MXene's concentration within the composite. When the composite features a notably high MXenes content in conjunction with MOs, the gas response of the composite sensor aligns with that of a pure MXenes sensor, and the composite sensor exhibits significantly lower resistance compared to a pure MO sensor.[80] In this scenario, the presence of MOs enhances the specific surface area and facilitates the adsorption of gases.[81] Conversely, in situations where the MXenes content is relatively low, the gas response of the composite sensor aligns with that of the MO sensor, and the composite sensor exhibits considerably higher resistance compared to a pure MXene sensor.[82] In this instance, the MO take on a central role in facilitating carrier conduction during the gas-sensing process.

5. Why MXene for sensing applications?

The integration of sophisticated nanomaterials has ushered in a new era in the realm of sensors. When it comes to the process of signal transduction, selecting the appropriate transducer (material) is of the utmost importance. Traditional transducers suffer from the necessity of a high over-potential in the case of electrochemical sensors because of their extremely small surface area. Additionally, the target analyte's slow charge kinetics and the mass transfer constraint make it difficult for the transducer to transfer enough mass. The materials for strain sensors, instead, must preserve conductivity and mechanical strength. As a result, any viable sensor device's transducer material should have significant properties such as high surface area and high conductivity, superior mechanical strength, and a simple synthesis process. To accomplish this, a wide

range of materials, including metals, polymers, metal oxides, and carbonaceous materials, as well as their combinations, have been investigated. The race to identify the ideal combination with a high signal throughput is still ongoing despite this. In 2011, Drexel University was credited with discovering MXenes, a novel type of 2D material.[30] Although their primary application is in the field of energy materials, such as batteries and supercapacitors, the community of sensor researchers is showing an unusual interest in these 2D materials.[83] The diversity of their surface and chemical properties is directly tied to the growing application of sensor technology, which is directly related to their increasing reach. MXenes have relatively high hydrophilicity and are simple to functionalize on the surface. This is in contrast to other 2D materials like graphene, which, despite having a high conductivity, is challenging to integrate with electrode systems due to its low hydrophilicity and the fact that its sheets can be folded or re-stacked.[84] In addition, because of their exceptionally high conductivity, MXenes are an excellent substrate for the research and development of electrochemical sensors.[33] Because of their superior mechanical qualities and conductivity, MXenes provide a great conductive filler that may be used in strain and pressure sensors. It is an attractive transducing material for various sensors due to MXenes' excellent surface characteristics, metal-like conductivity, and flexibility with just the right amount of stiffness. These characteristics make MXenes suitable for electrochemical, strain bio-electrochemical, photochemical, and pressure sensors.[85]

6. Application of $Ti_3C_2T_x$ MXene as a gas sensor

In order to make an accurate comparison of $Ti_3C_2T_x$ MXene's application in gas sensors, the nanomaterial can be divided into three distinct classes: pure $Ti_3C_2T_x$, functionalized $Ti_3C_2T_x$, and composite $Ti_3C_2T_x$. This review article investigates the functionalization of $Ti_3C_2T_x$ in terms of the alteration of functional groups and the intercalation of metal ions. Additionally, combining $Ti_3C_2T_x$ with other materials is a successful tactic to enhance its gas-sensing performance. There are many various subgroups of materials that can be composited with $Ti_3C_2T_x$, including transition-metal dichalcogenides (TMDs), graphene derivatives, metal oxides, polymers, *etc.* $Ti_3C_2T_x$ can be used to make a variety of different composites. The application in gas sensors of all three different categories of $Ti_3C_2T_x$ will be discussed one by one.

6.1 Pure $Ti_3C_2T_x$ for gas sensor

After the discovery of MXene in 2011, $Ti_3C_2T_x$ was initially used as a gas sensor, as reported by Lee *et al.*[75] They reported the $Ti_3C_2T_x$-based volatile organic compounds (VOC) gas sensor at room temperature by integrating the $Ti_3C_2T_x$ nanosheets with solution-processed on flexible polyimide film. At ambient temperature, the $Ti_3C_2T_x$ sensors demonstrated p-type sensing behaviour while successfully measuring methanol, ethanol,

acetone, and ammonia gas. The fabricated sensor exhibited the highest and lowest response when exposed to ammonia gas due to large adsorption energy, as shown in Fig. 4(b). Theoretically, the estimated value of the limit of detection (LOD) for acetone gas is 9.27 ppm. To detect VOC gases at parts per billion (10^{-9}) level, Kim *et al.* proposed a $Ti_3C_2T_x$ gas sensor with an extremely high signal-to-noise ratio (SNR).[74] They deposited a thin film of fully functionalized and high metallic conductivity of multi-layered $Ti_3C_2T_x$ on a pre-printed Au electrode SiO_2 substrate. The $Ti_3C_2T_x$ gas sensor's response and SNR were compared to those of typical 2D materials (including MoS_2, black phosphorus (BP), and reduced graphene oxide (r-GO)). It was revealed that the $Ti_3C_2T_x$ sensor's SNR was two orders of magnitude higher than that of other 2D materials because of their incredibly low noise level. $Ti_3C_2T_x$ MXene gas sensors showed a very low limit of detection (LOD) for VOC gases of 50–100 ppb at room temperature. A single-layer Ti_3C_2-based NH_3 sensor was proposed by Wu *et al.* at ambient temperature with high selectivity [Fig. 4(c) and (d)].[86] Following intercalation, ultrasonic dispersion, and delamination, Ti_3C_2 was coated on the ceramic tube's surface to make the gas sensor ready to detect a variety of gases, including NO, CH_4, NH_3, H_2S, H_2O, acetone ethanol, and methanol with 500 ppm concentration at room temperature. According to their research, the single-layer Ti_3C_2 sensor had the highest response, which was adequately explained by first-principles calculations. Several investigations on NH_3 showed that the manufactured Ti_3C_2-based sensors have good repeatability to ammonia at room temperature, with a detection limit of 10 ppm. Additionally, utilising practical first principles, Khakbaz *et al.* thoroughly investigated the possibility of pure $Ti_3C_2T_x$ for gas sensing.[87] On $Ti_3C_2T_x$, gas molecules such as NH_3, CO, N_2O, NO, NO_2, CH_4, CO_2, and H_2S were adsorbed, and the effects of various ratios of numerous functional groups were examined. The results showed that $Ti_3C_2T_x$ is especially sensitive to NH_3 relative to the other gas molecules studied, with a charge transfer of 0.098 *e* and adsorption energy of 0.36 eV, respectively. Using first-principles analysis, Zeng *et al.* also reported that $Ti_3C_2T_x$ MXene is foreseen to be an encouraging sensor for SF_6 decomposition characteristic components.[88] The adsorption strength of analytes is unevenly exhibited by different terminated $Ti_3C_2T_x$ MXene, and hydroxyl groups greatly enhance the adsorption strength on the $Ti_3C_2T_x$ MXene surface. Based on their finding they also suggested that following the adsorption of the analytes, a clear charge transfer is what primarily causes variations in $Ti_3C_2T_x$ conductivity.

Numerous variables, including film thickness, MAX phase precursors, flake size, and degree of oxidation, have an impact on the gas sensing capabilities of pure $Ti_3C_2T_x$.[89,90] For gas (acetone, ethanol, and NH_3) detection, Kim *et al.* also described an interfacial assembly of ultrathin $Ti_3C_2T_x$ films.[90] In particular, the addition of ethyl acetate to the $Ti_3C_2T_x$ solution promotes the production of a self-assembled layer, which had an excellent plane adhesion and stacking order. It was
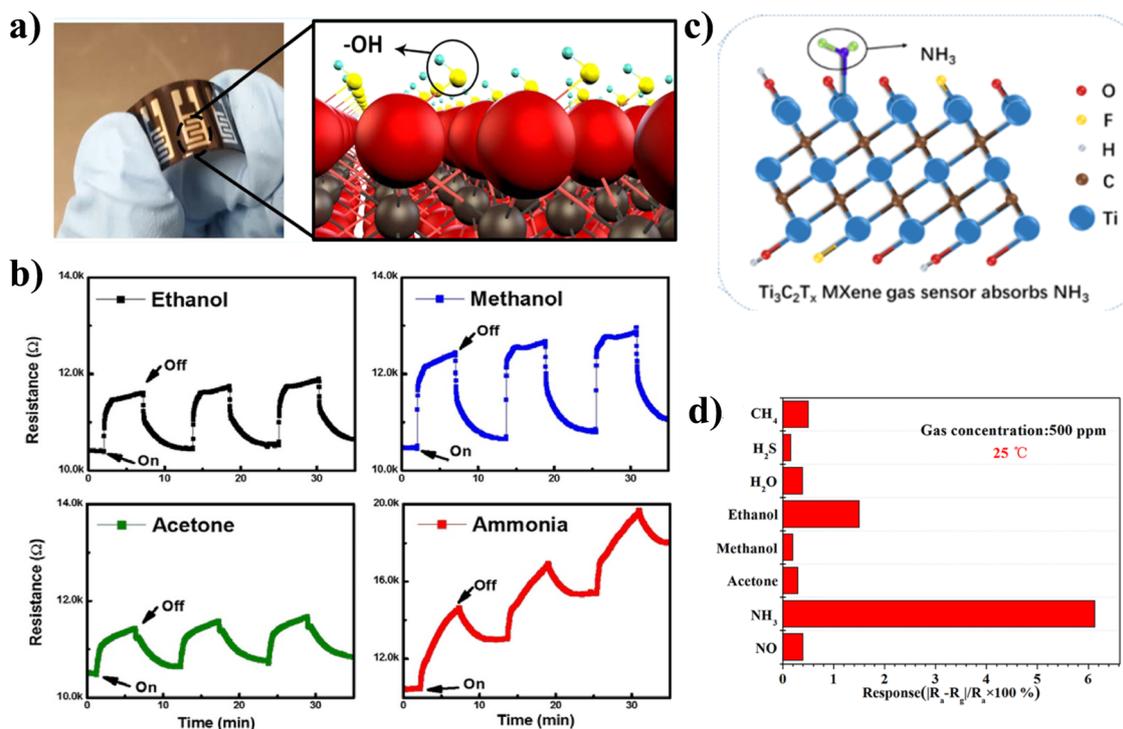
Fig. 4 (a) Schematic illustration of pure $Ti_3C_2T_x$ VOCs, (b) results of ethanol, methanol, acetone, and ammonia gas bubbling at 100 ppm using $Ti_3C_2T_x$ based sensor at 300 K. Reproduced with permission from ref. 75 Copyright 2017. American Chemical Society, (c) pictorial representation of absorption of NH_3 on the surface of $Ti_3C_2T_x$ MXene and, (d) room temperature response of Ti_3C_2 MXene gas sensors toward 500 ppm CH_4, H_2S, H_2O, ethanol, methanol, acetone, NH_3, and NO. Reproduced with permission from ref. 86 Copyright 2019. American Chemical Society.
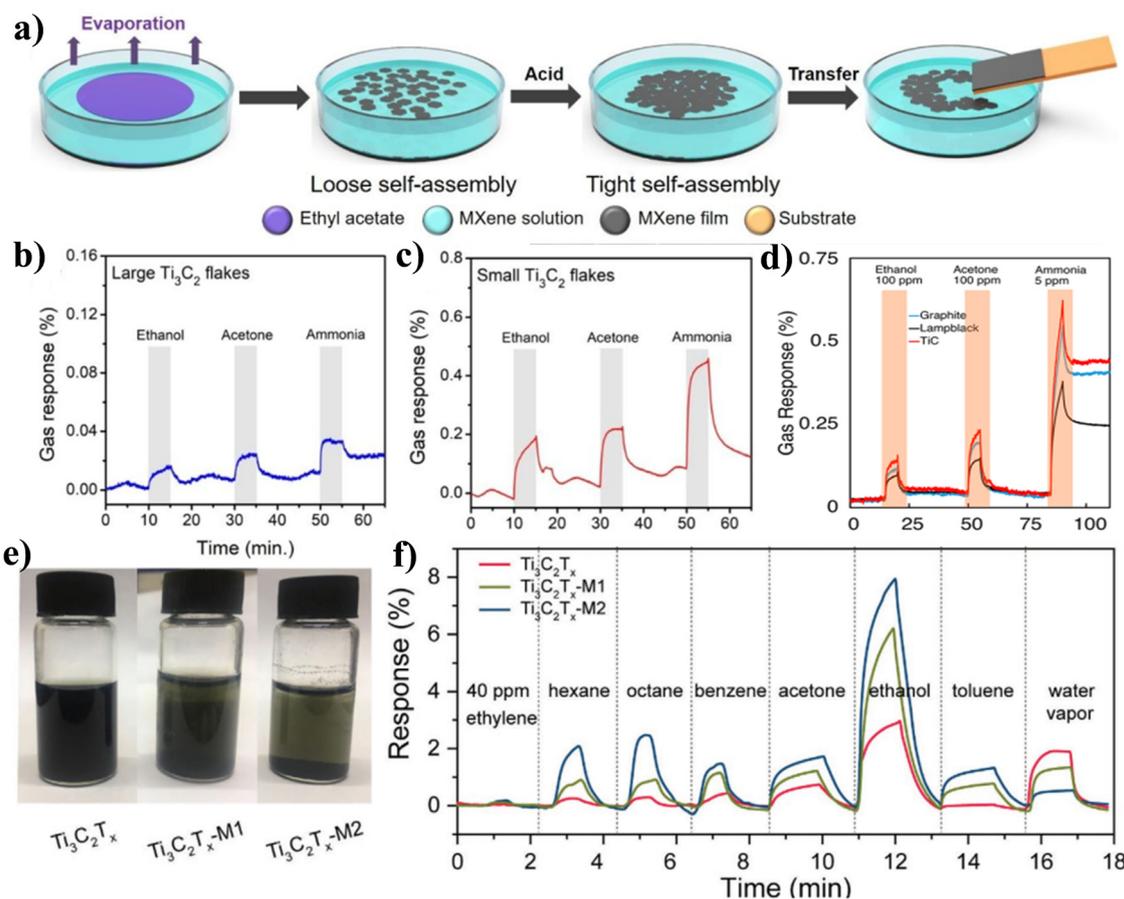
Fig. 5 (a) Schematic of the interfacial self-assembly technique for preparation of ultrathin MXene films. Gas sensing response of, (b) large Ti_3C_2 flakes, (c) small Ti_3C_2 flakes. Reproduced with permission from ref. 90 Copyright 2019. American Chemical Society, (d) $Ti_3C_2T_x$'s ability to detect gases after being made from various MAX precursors which showed different sensitivities with ethanol, acetone, and ammonia. Reproduced with permission from ref. 54 Copyright 2019. American Chemical Society, (e) photographs of pure $Ti_3C_2T_x$, $Ti_3C_2T_x$-M1, and $Ti_3C_2T_x$-M2 colloid solution and, (f) gas sensing performance of VOCs at 40 ppm concentration. Reproduced with permission from ref. 92 Copyright 2021. Wiley.

discovered that the self-assembly technique could improve the connectivity of small flakes, leading to minimal electrical noise in the gas sensor [Fig. 5(a) and (b)]. The gas sensor made of ultrathin $Ti_3C_2T_x$ responded to NH_3 the best, as shown in Fig. 5(c). According to research by Shuck et al., the MAX phase carbon sources had an impact on the $Ti_3C_2T_x$'s structure and characteristics.[54] The three different types of $Ti_3C_2T_x$ that were produced through etching varied in terms of chemical composition, lateral flake size, electrical conductivity, and stability. They reported that $Ti_3C_2T_x$ made from graphite had the highest conductivity (4400 S cm^{-1}) and was the most stable (time constant, 10.1 days), whereas MXene made from TiC had a similar conductivity (3480 S cm^{-1}) but had the lowermost colloidal stability (4.8 days) as well as the lowest chemical stability (5.1 days). The most responsive to gases and with good selectivity to NH_3 was the TiC-produced $Ti_3C_2T_x$, as shown in Fig. 5(d). In spite of this, $Ti_3C_2T_x$ has not made significant progress in the field of gas sensors due to the fact that it is easily oxidized and has a tendency to be unstable. Chae et al. looked into the key variables (including water molecules, temperature, and solvents) controlling the oxidation of $Ti_3C_2T_x$

in order to get around this constraint. They proposed that low temperature and ethanol solvent can help in maintaining the intrinsic properties of prepared $Ti_3C_2T_x$.[91] For the purpose of detecting VOCs at room temperature, Liu et al. recently proposed termination-modified $Ti_3C_2T_x$ MXene ($Ti_3C_2T_x$–M) through alkali pre-treatment and trimethylacetic anhydride functionalization [photograph is shown in Fig. 5(e)].[92] In comparison to its unprepared counterpart, the $Ti_3C_2T_x$ sensor showed a fivefold increase in response to ethanol with a 29% reduction in response to water vapor followed by the spray coating methods, as shown in Fig. 5(f).

In summary, one notable advantage of pristine $Ti_3C_2T_x$ MXene-based gas sensors is their exceptional sensitivity and rapid response to a wide range of gases. These sensors exhibit high surface area, enabling effective gas adsorption, and their 2D layered structure provides numerous active sites for gas molecules to interact with, resulting in enhanced detection capabilities. Additionally, MXene-based sensors often possess excellent electrical conductivity, facilitating quick and precise signal readouts. These properties make them highly versatile for gas sensing applications, ranging from environmental

monitoring to industrial safety, where the ability to detect and respond to diverse gas species swiftly and accurately is of paramount importance. However, one significant drawback of pristine $Ti_3C_2T_x$ MXene-based gas sensors is their limited selectivity when detecting multiple gases simultaneously. The inherent reactivity of MXene materials can lead to cross-sensitivity issues, making it challenging to distinguish between different gas species accurately. The MXene's hydrophilic nature can lead to water absorption, which interferes with gas sensing performance and reduces sensitivity. To overcome this limitation, researchers have been exploring strategies such as surface functionalization and composite material design, which we will discuss one by one in next section. Surface modification with specific functional groups or the incorporation of other nanomaterials can enhance the selectivity of MXene-based sensors by tailoring their chemical affinity to target gases. These advancements in MXene-based gas sensors hold promise for enhancing their practical utility in real-world applications.

6.2 Functionalized $Ti_3C_2T_x$ for gas sensor

Even though $Ti_3C_2T_x$ has metallic properties when it is pure, its electronic properties can be changed by functionalization and become semiconducting. The functionalization can be done through metal ion intercalation,[93] sulphur doping,[94] oxidation,[95] noble metal modification,[96] and functional group modification.[97,98] Researchers have started to pay more attention to functionalization because it can improve the adsorption effect of $Ti_3C_2T_x$, which is favorable for gas sensing applications. Metal ion intercalation was studied by Koh et al. as part of their investigation into how gas-induced interlayer swelling

of $Ti_3C_2T_x$ influences the performance of gas sensing.[93] When NaOH was utilized as the ionic intercalating agent, the in situ X-ray diffraction (XRD) experiments demonstrated a significant relationship between the gas response and the interlayer transport caused by the interlayer ions as shown in Fig. 6(a). The highest level of sensitivity was reported in $Ti_3C_2T_x$ after treatment with 0.3 mmol L^{-1} NaOH, and the highest response was achieved for ethanol, as shown in Fig. 6(b). Similar to this, Yang et al. enhanced the gas sensing performances of the organ-like $Ti_3C_2T_x$ by –OH functional alteration and alkaline metal ion (Na) intercalation.[79] The sensing components were uniformly coated on the Al_2O_3 ceramic substrate by drop-coating process to create the pristine $Ti_3C_2T_x$ and alkalized $Ti_3C_2T_x$ gas sensors to study the alkalized $Ti_3C_2T_x$'s gas sensing performance and the schematic is shown in Fig. 6(c). It was discovered that the alkalized $Ti_3C_2T_x$ exhibited the opposite tendency to the pristine $Ti_3C_2T_x$, whose resistance rose with the concentration of NH_3. The highest response with alkalized $Ti_3C_2T_x$ was achieved in NH_3 gas (around 28.7% more than pristine $Ti_3C_2T_x$) and the selectivity also enhanced with alkalized $Ti_3C_2T_x$ (ethanol, acetaldehyde, formaldehyde, methanol, acetone, methane, and NO_2) as shown in Fig. 6(d).

The inherently metallic $Ti_3C_2T_x$ was functionalized with oxygen by Pazniak et al. to increase gas sensitivity. Fig. 7(a)–(g)[95] shows that Ti_3C_2T had been partially oxidized kept its conductivity at the optimum annealing temperature of 350 °C, and the TiO_2 formed during oxidation improved its detection capacities to gases at concentrations as low as 10^{-6}. The partially oxidized multisensor array-based $Ti_3C_2T_x$ demonstrated strong response values and selectivity for acetone. Recently, Yao et al. also demonstrated a partially oxidized $Ti_3C_2T_x$ MXene-based sensor which
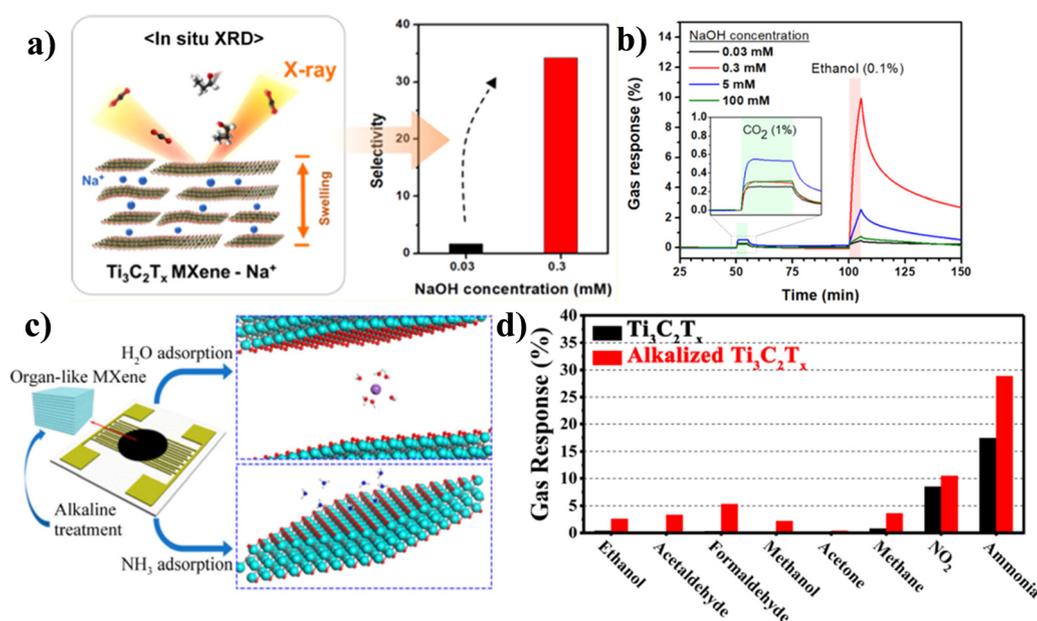

Fig. 6 (a) Gas sensor schematic based on $Ti_3C_2T_x$, where mM stands for mmol L^{-1}, (b) gas response of $Ti_3C_2T_x$ sensors with different concentrations of NaOH, inset: magnified gas response of CO_2. Reproduced with permission from ref. 93 Copyright 2019. American Chemical Society, (c) schematic of an organ-like $Ti_3C_2T_x$-based gas sensor with alkaline treatment, (d) selectivity test of alkalized $Ti_3C_2T_x$ and $Ti_3C_2T_x$ with a 100 ppm concentration to various test gases. Reproduced with permission from ref. 79 Copyright 2019. American Chemical Society.

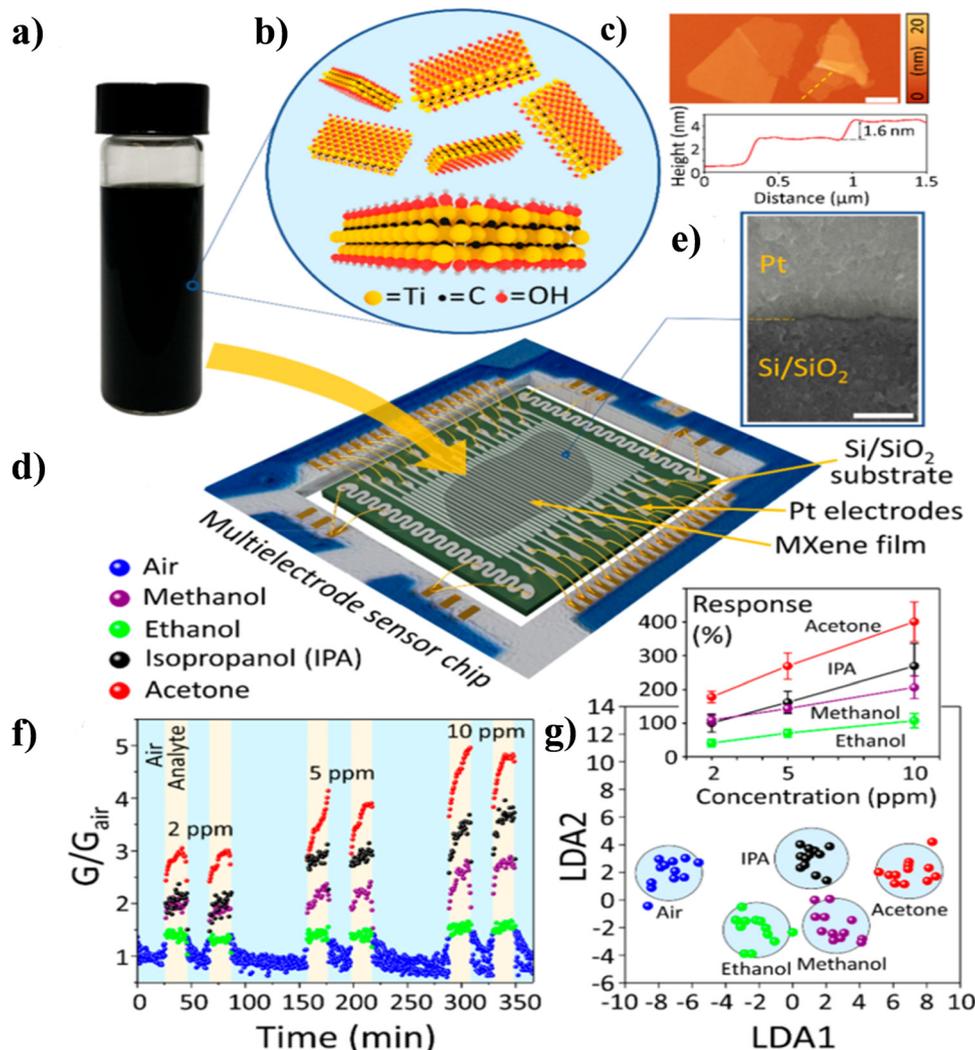**Fig. 7** A partially oxidised $Ti_3C_2T_x$ MXene film's gas sensing capabilities on a multisensor chip: (a) image of a water-based, stable delaminated MXene solution, (b) monolayer $Ti_3C_2T_x$ MXene flakes' schematic structure, (c) $Ti_3C_2T_x$ MXene flakes on Si/SiO₂ as depicted in an AFM image with scale bar 1 μm, (d) schematic of a multielectrode chip with a coating of drop-cast MXene flakes, (e) SEM image of a MXene film with contact area between Si/SiO₂ substrate and Pt electrode, (f) variation of MXene $G/(G_{air})$ with time, (g) the multisensor array vector signals are anticipated by LDA into a two-component taste diagram for three organic vapours (10 ppm) and dry air; the circles associated to the gases are constructed with a 0.7 confidence around the relevant gravity centres (Main figure), dependence of the chemiresistive response with different concentration of gases (inset). Reproduced with permission from ref. 95 Copyright 2020. American Chemical Society.

showed a high response and excellent selectivity for NH_3.[99] The heat treatment of the detecting ceramic tube, which eliminates the adsorbed water and partially oxidizes the material at a temperature of 280 °C, is an essential aspect of this work. The $Ti_3C_2T_x$ MXene-280 has a 147% response to 500 ppm NH_3 in ambient conditions, whereas the equivalent response/recovery time are 67/157 s, respectively.[99]

The electrochemical performance of the 2D $Ti_3C_2T_x$ sheet decorated with Pt nanoparticles (PtNPs) was studied by Lorencova *et al.*[100] The findings demonstrated that $Ti_3C_2T_x$/PtNP nanocomposite exhibited significantly superior and more stable redox activity in an anodic potential window compared to GCE treated with pure $Ti_3C_2T_x$ MXene. The H_2O_2 sensor fabricated with $Ti_3C_2T_x$/PtNP on GCE provided LOD of 448 nM

and a potential at which reduction begins of +250 mV (*vs.* Ag/AgCl), in contrast to 883 M and 160 mV observed for $Ti_3C_2T_x$ modified GCE. A flexible hydrogen sensor was also fabricated by Zhu *et al.*, employing $Ti_3C_2T_x$ MXene that had been modified with the noble metal palladium (MXene@Pd CNC).[96] This sensor had a response time of (32 ± 7) s and a sensitivity range of $S = (23 \pm 4)\%$ to 4% H_2.

In summary, functionalized $Ti_3C_2T_x$ MXenes hold great promise for gas sensors due to their versatility and tunable surface chemistry, offering distinct advantages and potential drawbacks. One significant advantage is their enhanced selectivity and sensitivity towards specific gases. By introducing functional groups like –OH, –F, or –NH₂, the MXene surface can be tailored to interact selectively with target gas molecules,

leading to improved detection capabilities for specific gases of interest. Moreover, functionalization can increase the active sites available for gas adsorption, further enhancing sensitivity. However, a notable drawback of excessive functionalization is the potential reduction in electrical conductivity. This can hinder electron flow within the sensor, impacting its overall performance. To overcome this limitation, researchers are actively working on optimizing the degree of functionalization to strike a balance between improved selectivity and maintaining good conductivity. Additionally, innovative techniques such as *in situ* functionalization and the development of hybrid structures that combine functionalized and pristine MXenes are being explored. These approaches aim to harness the benefits of functionalization while mitigating its negative impact on conductivity, thereby ensuring the gas sensor's overall effectiveness. Furthermore, the integration of functionalized MXenes into composite materials or heterostructure with other conductive materials like graphene or carbon nanotubes has shown promise in overcoming conductivity challenges while preserving the enhanced gas-sensing properties. In brief, functionalized $Ti_3C_2T_x$ MXenes offer tailored selectivity in gas sensors, but careful consideration of conductivity issues and the exploration of hybrid structures and composite materials are essential for optimizing their performance in practical applications.

6.3 $Ti_3C_2T_x$ composites-based gas sensor

A key tactic to enhance the gas sensing capabilities of $Ti_3C_2T_x$ is the formation of the composite. The diversity of materials, including metal oxides,[101] TMDs,[102] graphene[103] and polymers,[104] have been effectively combined with $Ti_3C_2T_x$. The $Ti_3C_2T_x$ composite-based gas sensor attracts much attention because of the formation of a Schottky barrier due to the combination of metal oxide and $Ti_3C_2T_x$, which improves the gas sensing performance of the device. To advance the NH_3 sensing properties of pure $Ti_3C_2T_x$, Tai et al. reported a gas sensor based on a bilayer film of TiO_2 and $Ti_3C_2T_x$.[81] In accordance with the findings, the $TiO_2/Ti_3C_2T_x$ sensor responds to 10 ppm NH_3 at room temperature with a response value that is 1.63 times greater and response/recovery times that are 0.65 and 0.52 times faster than those of a pure $Ti_3C_2T_x$ sensor as shown in Fig. 8(a) and (b). The $TiO_2/Ti_3C_2T_x$ sensor, meanwhile, has an excellent linear response ($R^2 = 0.95596$) at NH_3 concentrations of 2 to 10 ppm and can detect NH_3 concentrations as low as 0.5 ppm. Sun et al. demonstrated how to synthesise $W_{18}O_{49}/Ti_3C_2T_x$ composites using an easy solvothermal technique to grow 1D $W_{18}O_{49}$ nanorods (NRs) on $Ti_3C_2T_x$ MXene sheets as shown in Fig. 8(c).[105] The reported $W_{18}O_{49}/Ti_3C_2T_x$ composites have excellent selectivity, enduring stability, a low LOD (170 ppb acetone), and quick response and recovery time (5.6 s and 6 s to 170 ppb acetone). They also reported a good response to low concentrations of acetone (11.6 to 20 ppm) and the operated temperature of the device was 300 °C as shown in Fig. 8(d).

TMDs have received attention as prospective composite materials because of their numerous redox reaction active sites

and high surface reactivity. To enhance the sensing capabilities of TMDs at ambient temperature, MXene can be combined with other TMDs, including In_2O_3, WS_2, SnO_2, graphene, CoS, WSe_2, and MOS_2, to generate heterojunctions.[39,102,106–110] $Ti_3C_2T_x$ and WSe_2 were the model materials that Chen et al. decided to use in their implementation of the detection of various volatile organic compound (VOC) gases.[102] The nanohybrids gas sensor based on $Ti_3C_2T_x/WSe_2$ was synthesized by combining liquid-phase exfoliation $Ti_3C_2T_x$ with WSe_2 that had been functionalized with cetyltrimethyl ammonium bromide (CTAB), as shown in Fig. 9(a) and (b). The gas sensor that was fabricated employing inkjet printing materials and a wireless monitoring system displayed a 12-fold improvement in ethanol sensitivity, very fast response and recovery time (9.7 s and 6.6 s), and a very low level of electrical noise. In addition, graphene and its derivatives have been the subject of a significant amount of research owing to the high surface area of these materials and the fact that their conductivity can be controlled. As a result, composites made of graphene and $Ti_3C_2T_x$ are deserving of future investigation in the realm of gas sensing. Yuan et al. have demonstrated a VOC sensor that is both high-performing and versatile, and it is built on a 3D MXene framework (3D-M).[111] The 3D-M was fabricated by combining a robust electrospinning method. The 3D-M sensor is able to function at ambient temperature thanks to its extremely interconnected porous structure. It is especially sensitive to extremely low concentrations of volatile organic compounds (ppb level) due to its capacity to quickly access and disperse gas molecules. In addition, the sensor has a very wide sensing range, a quick response and recovery time (less than two minutes), and excellent reversibility and versatility for a variety of volatile organic compounds. The researchers led by Lee et al. announced the fabrication of $Ti_3C_2T_x$ MXene/graphene hybrid fibres by a wet-spinning approach.[112] The remarkable mechanical and electrical qualities of these hybrid fibers make them ideally suited for use in flexible wearable gas sensors. The ability of the produced fibers to demonstrate significant sensitivity to NH_3 gas at ambient temperature is made possible by the synergistic impacts of the electrical characteristics and gas-adsorption capacities of MXene and graphene. In comparison to MXene and graphene on their own, the hybrid fibers demonstrated an NH_3 sensing response that was 6.77% more sensitive ($\Delta R/R_0 = 6.77\%$). Even after being bent over a period of 2000 times, the hybrid fibres showed an exceptionally high degree of mechanical flexibility, with a resistance that changed by $\pm 0.2\%$ and a low level of noise resistance. This enabled the hybrid fibres to detect gas even as they were deformed, as shown in Fig. 9(c) and (d). Recently, Yang et al. demonstrated the inherent process of the improvement of gas-sensing capabilities of oxidized $Ti_3C_2T_x$ by analyzing the performance of crumpled $Ti_3C_2T_x$ spheres.[113] This was done in order to show that the crumpled $Ti_3C_2T_x$ spheres have better gas-sensing properties. After explaining the structural and compositional modifications caused by the oxidation of $Ti_3C_2T_x$, it was found that the increase in gas-sensing capabilities was due to the presence of a large number of Ti atom defects that had been introduced by the
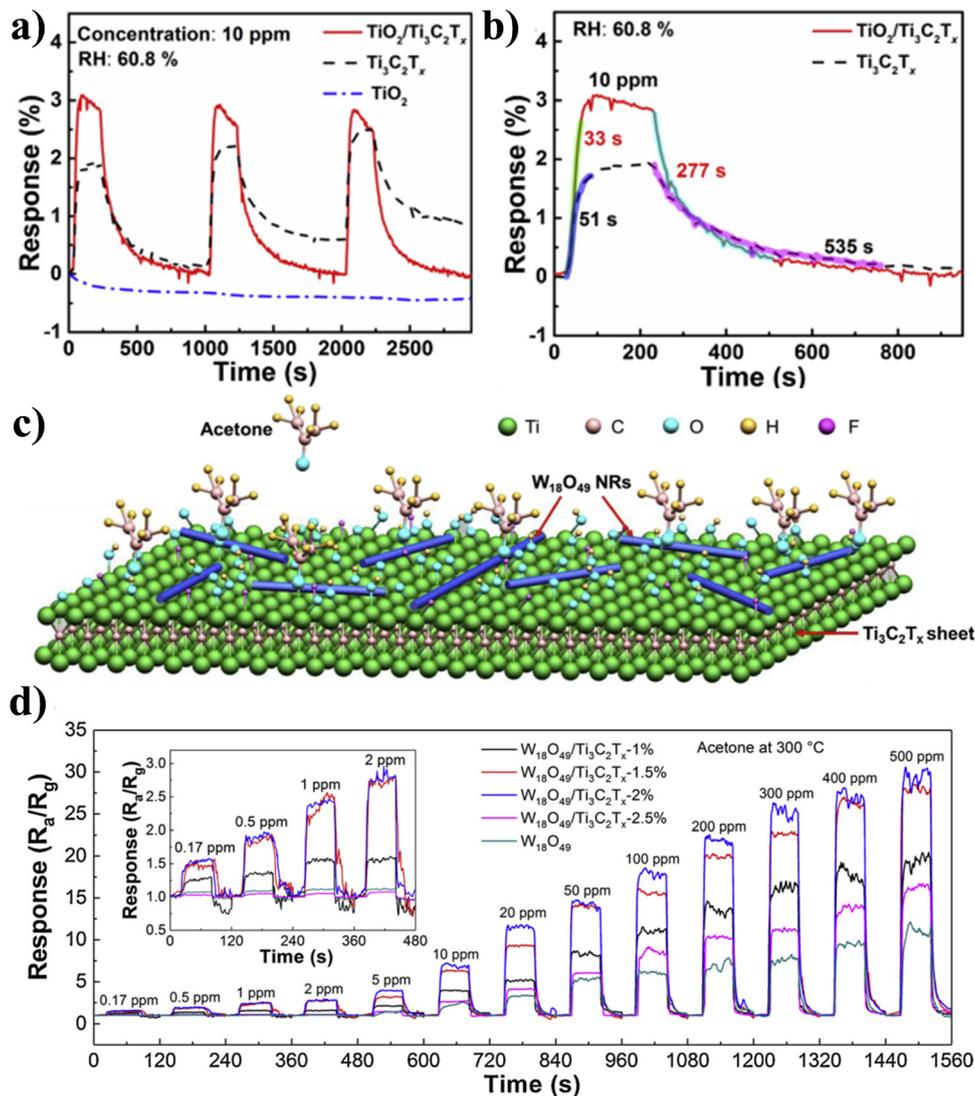
Fig. 8 (a) Response/recovery curve at a concentration of 10 ppm NH_3 for $TiO_2/Ti_3C_2T_x$, $Ti_3C_2T_x$, and TiO_2 gas sensors, (b) response and recovery times of the $Ti_3C_2T_x$ and $TiO_2/Ti_3C_2T_x$ gas sensors. Reproduced with permission from ref. 81 Copyright 2019. Elsevier, (c) schematic of reaction between acetone and $Ti_3C_2T_x/W_{18}O_{49}$ composite and (d) response–recovery curves of different sensors at a concentration of 0.17–500 ppm acetone at 300 °C temperature, Inset: Response–recovery curves towards 0.17–2 ppm acetone (enlarged view). Reproduced with permission from ref. 105 Copyright 2019. Elsevier.

oxidation process. This was discovered after it was established that oxidation had brought about changes in structure and composition. Calculations using the first principles of density functional theory (DFT) were carried out, and the findings revealed that the adsorption capacity of Ti atom defect sites for gas molecules was significantly improved, particularly with respect to NO_2. Meanwhile, a reducing agent known as $Ti_3C_2T_x$ was utilized to assist in the process of GO reduction. The gas sensing performance was further improved by forming a $Ti_3C_2T_x/TiO_2/rGO$ heterostructure, which resulted in high sensitivity, low level of detection limit, and a remarkable selectivity to NO_2, reaching up to 19.85% for 5 ppm NO_2 at ambient temperature. All of these improvements were made possible by the formation of the heterostructure.

Since polymers are sensitive, cheap, versatile, and may be used at room temperature, they have frequently been used to

fabricate $Ti_3C_2T_x$ composites. Flexible gas sensors based on the $Ti_3C_2T_x$/polyaniline (PANI) nanocomposite were studied by Zhao et al. using density functional theory in conjunction with electrosensitive experiments on large samples.[104] This composite sensing material showed a high sensitivity for ethanol (41.1% at 200 ppm) and fast response/recovery time (0.4/0.5 second) at room temperature, as shown in Fig. 10(a) and (b), which makes it the next-generation sensing material that can quickly detect real-time VOC gases. This is because the properties of composites and highly active $Ti_3C_2T_x$ MXene work synergistically with one another. To track NH_3 volatilization in farming operations, Li et al. report the development of a polyaniline (PANI)/$Ti_3C_2T_x$ hybrid sensitive film-based flexible chemiresistive gas sensor.[114] An in situ method of self-assembly was utilized during the process of depositing the hybrid film
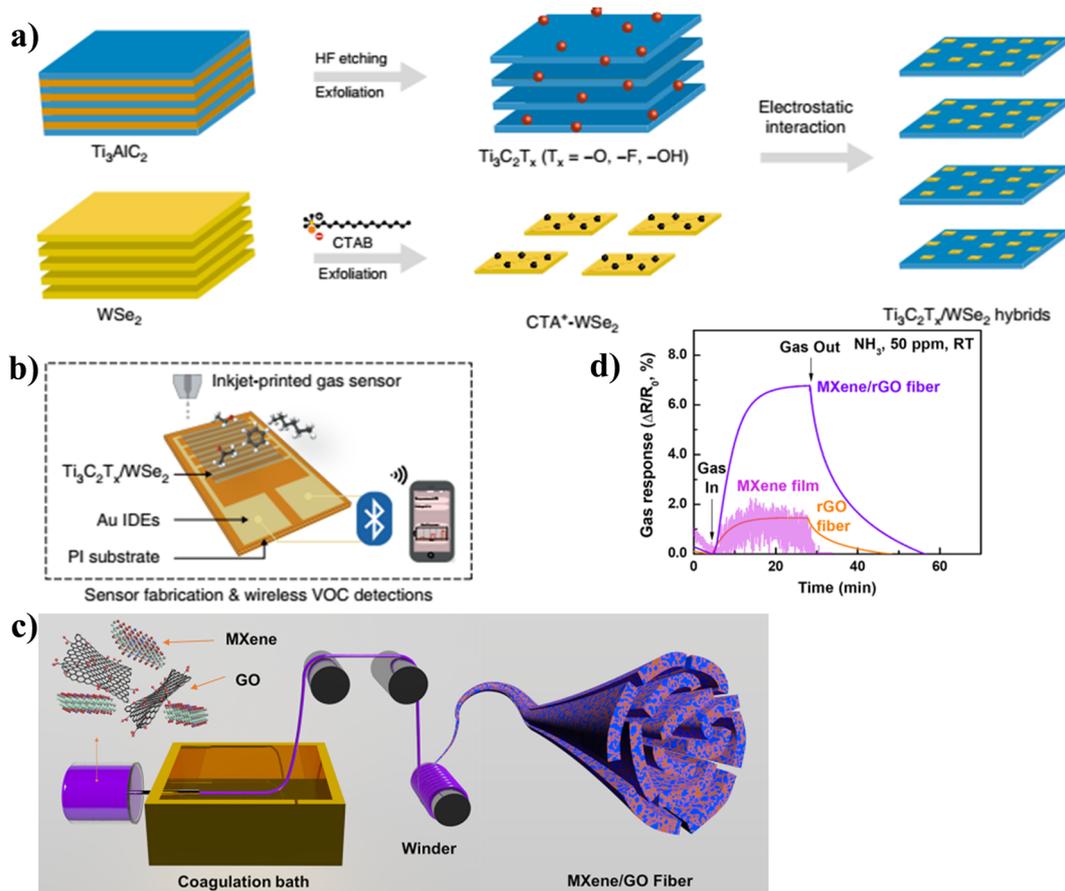
Fig. 9 (a) A schematic representation of the steps involved in the preparation of $Ti_3C_2T_x$/WSe_2 nanohybrids, (b) illustration of inkjet-printed gas sensors for the detection of VOC using a wireless monitoring system. Reproduced with permission from ref. 102 Copyright 2020. Springer Nature (Open Access), (c) schematic of the spinning process for MXene/GO hybrid fiber, and (d) comparison of the gas response of MXene film, rGO fiber, and MXene/rGO hybrid fiber (40 wt% MXene). Reproduced with permission from ref. 112 Copyright 2020. American Chemical Society.

onto the flexible polyimide substrate, as shown in Fig. 10(c). High sensitivity, excellent repeatability, a low detection limit, and strong air stability are all characteristics of this sensor, which is enabled by the gas-sensing enhancing effects of the PANI/$Ti_3C_2T_x$ Schottky junction and the enhanced protonation degree of PANI in the hybrids. Particularly, the sensor demonstrates outstanding NH_3-sensing properties in situations with relative humidity (RH) of 20–80% at a 10–40 °C temperature range. This makes it attractive for real-world agricultural applications because it can operate in a wide temperature range. Wang *et al.* investigated the possibility of using a conductive poly(3,4-ethylenedioxythiophene) doped with poly(styrene sulfonic acid) (PEDOT:PSS) composite $Ti_3C_2T_x$ in a gas sensing application, as shown in Fig. 10(d).[115] In comparison to the pristine materials, the $Ti_3C_2T_x$/PEDOT:PSS sensor, which was fabricated using the process of drop-coating, exhibited superior sensing behaviors when exposed to VOC vapors at ambient temperature. They also investigated the effect of composite ratio on gas sensing performance, and the findings revealed that the ideal mass ratio for PEDOT:PSS and $Ti_3C_2T_x$ was 4:1. This ratio produced the maximum response from both of these gas sensing components. Recently, Chen *et al.* reported a

nanocomposite of $Ti_3C_2T_x$ MXene and polypyrrole (PPy) by using *in situ* polymerization reaction for gas sensing application.[116] The PPy/MXene-12, a nanocomposite-based gas sensor, displayed the best possible gas-detecting performance. It had a high response of 31.9% to 100 ppm NH_3, a low detection limitation, and unfailing selectivity.

In summary, the $Ti_3C_2T_x$ composites-based gas sensors offer a range of advantages and drawbacks, necessitating innovative solutions for their optimal performance. One significant advantage is their improved conductivity and stability compared to pristine $Ti_3C_2T_x$, making them highly suitable for practical gas sensing applications. These composites often integrate $Ti_3C_2T_x$ with other materials like polymers, MOs, or carbon-based nanomaterials, harnessing the synergistic effects of each component. This enhances the sensor's electrical properties and provides a larger surface area for gas adsorption, leading to enhanced sensitivity and response times. However, a notable drawback is the potential loss of selectivity when using composites, as the additional materials may introduce cross-sensitivity to various gases. To address this, researchers are actively developing advanced composites with tailored properties that maintain or even improve selectivity while preserving
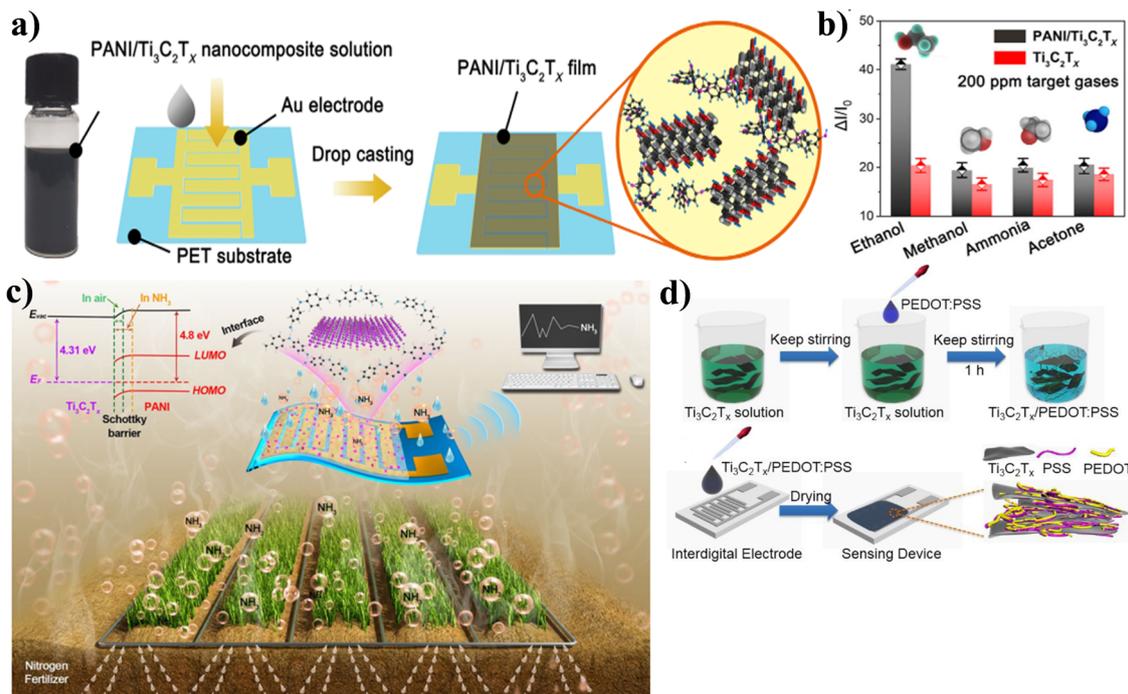
Fig. 10 (a) Interdigitated electrode schematic before and after coating with PANI/Ti$_3$C$_2$T$_x$ nanocomposites, (b) selectivity of Ti$_3$C$_2$T$_x$ and PANI/Ti$_3$C$_2$T$_x$-based flexible sensors exposed to 200 ppm. Reproduced with permission from ref. 104 Copyright 2019. John Wiley & Sons (Open Access), (c) agricultural NH$_3$ volatilization monitoring based on Ti$_3$C$_2$T$_x$/PANI NH$_3$ sensor. Reproduced with permission from ref. 114 Copyright 2020. Elsevier, (d) schematic of fabrication of Ti$_3$C$_2$T$_x$/PEDOT:PSS materials and gas sensor devices. Reproduced with permission from ref. 115 Copyright 2020. Elsevier.

high conductivity. Surface modification techniques and precise control over the composition and morphology of the composite materials allow for a fine-tuning of gas-sensing characteristics. Another challenge lies in the potential degradation of the composites over time due to environmental factors or harsh operating conditions. To overcome this, protective coatings or encapsulation techniques are being explored to shield the sensitive composites from external influences, thus improving their long-term stability and reliability. Moreover, ongoing research into the optimization of composite fabrication processes and the development of novel composite combinations are continuously pushing the boundaries of gas sensor technology, aiming to strike a balance between enhanced performance and selectivity, as well as long-term durability for a wide range of gas detection applications.

Recently, lots of research going on Ti$_3$C$_2$T$_x$ MXene based self-powered gas sensor. One of the most remarkable aspects of MXene-based gas sensors is their ability to operate without the need for external power sources, such as batteries. This is achieved through the concept of self-powering, where the interaction between the gas molecules and the MXene-based sensing layer generates electricity. Two primary mechanisms have been explored for self-powering MXene-based gas sensors.

(1) Piezoelectric effect: when gas molecules adsorb or react with the MXene surface, they induce mechanical deformation or strain in the sensing layer. This strain can be harvested as piezoelectric energy, which is then converted into an electrical

signal. This approach allows for the continuous and sustainable operation of gas sensors without the need for batteries.

(2) Triboelectric effect: in the triboelectric effect, friction or contact between the gas molecules and the MXene surface generates static electricity. This effect can also be harnessed to power gas sensors. As gas molecules interact with the MXene layer, they create charge imbalances that can be tapped into for sensing purposes.

Sardana et al. reported a self-powered humidity sensor using an electrospun anisotropic triboelectric nanogenerator (A-TENG) composed of aligned Ti$_3$C$_2$T$_x$ MXene nanofibers (NFs) and cellulose acetate (CA) NFs.[117] Significantly, anisotropic structure of TENG displays its potential in sensitive moisture detection upon fast adsorption/desorption of water molecules due to increased pore length of prepared NFs. They also demonstrated the applied application of detecting the skin moisture. The same group also reported, a new kind of MXene/TiO$_2$/C-NFs heterojunction-based sensory component for detection of NH$_3$ by using cellulose nanofibers (C-NFs) as a substrate. At room temperature, the proposed sensor shows excellent reproducibility, high selectivity, and sensitivity toward NH$_3$ (1–100 ppm) along with a fast response/recovery time (76 s/62 s).[118] Wang et al. demonstrated self-powered and low-temperature resistant Ti$_3$C$_2$T$_x$ MXene-modified electronic-skin (e-skin) for multifunctional sensing.[119] The reported e-skin displays decent sensitivity to pressure 8(1.29 mV Pa^{-1}) and frequency (5.60 V Hz^{-1}) at a low temperature (−15 °C). In the meantime, utilizing this flexible e-skin, they successfully demonstrated temperature sensing over the range

from −15 °C to 25 °C with a sensitivity of 76.6 nA cm^{-2} °C^{-1}. Gasso et al. reported SnO$_2$/Ti$_3$C$_2$T$_x$–MXene nanocomposite-based self-powered gas sensor for NO$_2$ sensing. The fabricated sensor has detection limit of 0.03 ppb NO$_2$ and power consumption as low as 1.2 μW. Moreover, they also reported SnO$_2$/MXene nanocomposite-based piezoelectric pressure sensor (PPs) with a high sensitivity of 2.088 kPa^{-1} under the pressure range of 1.63–6.23 kPa with a fast response time (265 ms) and recovery time (75.5 ms).[120] Wang et al. reported high-performance Ti$_3$C$_2$T$_x$ MXene/tungsten oxide nanofibers-based NO$_2$ sensor. The as fabricated self-powered Ti$_3$C$_2$T$_x$ MXene/WO$_3$ sensor driven by TENG has an outstanding response at room temperature (ΔU$_s$/U$_{sa}$ = 510% at 50 ppm) for NO$_2$ gas, which is 15 times larger than that of the resistive MXene/WO$_3$ sensor.[121]

While MXene-based self-powered gas sensors have made significant strides, ongoing research is focused on further enhancing their sensitivity, selectivity, and stability. Additionally, efforts are underway to reduce production costs and facilitate large-scale manufacturing for wider adoption. In conclusion, MXene-based self-powered gas sensors are poised to play a pivotal role in shaping the future of gas detection technology. Their unique combination of material properties, self-powering mechanisms, and diverse applications make them a promising solution for addressing environmental, industrial, and healthcare challenges. As research in this field continues to evolve, we can anticipate even more sophisticated and accessible MXene-based gas sensors that contribute to a safer and healthier world.

7. MXene gas sensor: theoretical approach

The intricacy of the sensing mechanism employed by MXene sensors introduces considerable difficulties when attempting to fine-tune them through experimental methods. MXene sensors are equipped with a sophisticated and multifaceted system for detecting various environmental changes or target analytes, and this complexity can make it a formidable task to optimize their performance through practical experimentation. This complexity arises from the intricate interplay of materials and physical processes within the sensor, requiring a deep understanding of its underlying principles to effectively modify and enhance its sensing capabilities. Consequently, researchers face significant challenges in achieving the desired sensor performance due to the complicated nature of the MXene sensing mechanism, which necessitates a meticulous and thorough approach to experimentation and tuning. Hence, there exists a requirement for atomic-level modeling, specifically utilizing techniques such as density functional theory (DFT) and molecular dynamics (MD), to complement the empirical data and advance our understanding of the interactions between MXene materials and gas analytes.

The first computational study was conducted by Yu et al., who demonstrated the potential of MXenes as a gas sensor using monolayer Ti$_2$CO$_2$.[122] They investigated the interaction behavior of H$_2$, N$_2$, CO$_2$, CO, NH$_3$, O$_2$, NO$_2$, and CH$_4$ gas

molecules on the semiconductor Ti$_2$CO$_2$. Because Ti$_2$CO$_2$ is the only one among its counterparts [Ti$_2$C, Ti$_2$CF$_2$, and Ti$_2$C(OH)$_2$] that exhibits semiconductor properties, the researchers focused their investigation on Ti$_2$CO$_2$ through first-principles simulations. Out of all the gases studied, NH$_3$ is the sole gas that chemisorbs onto the surface of the Ti$_2$CO$_2$ MXene. It accomplishes this by donating a relatively substantial charge of 0.174 e and establishing a N–Ti bond. In DOS analysis, there is a significant overlap of electronic charges, leading to orbital mixing and substantial charge transfer between NH$_3$ and Ti$_2$CO$_2$. This observation strongly indicates chemisorption, where chemical bonds are formed between NH$_3$ and Ti$_2$CO$_2$. Conversely, when examining other gas molecules, it was evident that they exhibited significantly lower gas adsorption energies and charge transfer compared to NH3. This points to the absence of overlapping electronic charges and signifies weak interactions between these molecules and the Ti$_2$CO$_2$ surface. The adsorption energy of NH$_3$ on Ti$_2$CO$_2$ was determined to be −0.37 electron volts (eV), which is quite less as compared to Ti$_2$C(OH)$_2$ [−0.48 eV], V$_2$CO$_2$ [−0.81 eV] and analogous to Ti$_3$C$_2$O$_2$ [−0.34]. The higher sensitivity of Ti$_2$CO$_2$ toward NH$_3$ was confirmed by calculating I–V curves before and after absorption of gas. Xiao et al. investigated the interactions of various gases, including NO, CO, H$_2$, CO$_2$, O$_2$, N$_2$, and CH$_4$, with Zr$_2$CO$_2$ MXene.[123] Their findings revealed that NH$_3$ exhibited strong chemisorption characterized by a noticeable charge transfer 0.188 e and a substantial adsorption energy −0.81 eV, whereas other gases were primarily physisorbed. The authors anticipated a similar response for M$_2$CO$_2$ (where M = Sc, Ti, Zr, and Hf) due to their analogous atomic and electronic structures. Additionally, it was observed that the transition from chemisorption to physisorption in NH$_3$ adsorption on Zr$_2$CO$_2$ occurred when two additional electrons were introduced into the MXene sheet, offering a practical means to release the gas molecule. In a subsequent study, Wang et al. conducted a comprehensive analysis of Hf$_2$CO$_2$'s performance in detecting multiple gases, including H$_2$, O$_2$, NO$_2$, SO$_2$, CO, CO$_2$, HCN, NH$_3$, and H$_2$S.[124] Consistent with the earlier report, Hf$_2$CO$_2$ exhibited remarkable sensitivity and selectivity toward NH$_3$, characterized by an exceptional charge transfer of 0.146 e and substantial adsorption energy of −0.834 eV. Additionally, it was observed that preadsorption of the MXene surface with H$_2$O, SO$_2$, and CO$_2$ molecules significantly enhanced NH$_3$ adsorption by fostering the formation of hydrogen bonds.

In addition to their experimental investigations, Kim et al. conducted a detailed examination of how the functional groups of Ti$_3$C$_2$T$_x$ MXene influence its sensing capabilities.[74] Employing the DFT approach, they analyzed the interactions between acetone and NH$_3$ with Ti$_3$C$_2$T$_x$ surfaces terminated by –OH, –O, and –F groups. Their findings indicated that Ti$_3$C$_2$(OH)$_2$ exhibited stronger binding energy with both acetone and NH$_3$ compared to Ti$_3$C$_2$O$_2$ and Ti$_3$C$_2$F$_2$ MXenes. Hajian et al. investigated the impact of the ratio of functional groups on NH$_3$ detection using Ti$_3$C$_2$T$_x$ MXene.[125] They examined two different ratios of –F functional groups in and observed that lower ratios of –F groups led to stronger NH$_3$ adsorption. This effect was

attributed to the smaller charge transfer between NH_3 and fluorine in comparison to NH_3 and oxygen. Consequently, the synthesis method and the choice of MAX phase etchant, which dictate the functional group ratios, emerged as critical factors influencing the gas-sensing performance of MXene sensors. Zhang et al. examined the ability of $Ti_3C_2O_2$ nanosheets to capture formaldehyde effectively at room temperature.[126] The findings revealed a moderate adsorption energy of 0.45 eV and an adsorption capacity exceeding 6 mmol g^{-1}, indicating the promising potential of $Ti_3C_2O_2$ MXene for indoor formaldehyde removal. Ma et al. explored M_2CO_2 (where M = Sc, Ti, Zr, and Hf) MXenes to identify the most effective platforms for detecting toxic SO_2.[127] Their investigation revealed that monolayer Sc_2CO_2 exhibited a robust chemical bond with SO_2, characterized by an adsorption energy of −0.646 eV and a charge transfer of 0.453 e, establishing it as a favorable material for SO_2 sensing. The M_2CO_2 MXene was also explored for other gas detection such as NO and CO. Regarding NO, the most significant interactions were observed between the molecule and Sc_2CO_2, likely due to orbital hybridization occurring between the MXene and the gas molecule near the Fermi level. This was substantiated by a substantial charge transfer of 0.303 e and a reasonably moderate adsorption energy of −0.47 eV, affirming Sc_2CO_2 as a highly suitable material for NO sensing. Conversely, in the case of CO, it was primarily physisorbed onto Sc_2CO_2 MXene, with a minimal charge transfer of 0.017 e. However, the sensing capabilities of Sc_2CO_2 MXene for CO were enhanced through the introduction of Mn dopants into the structure, resulting in a charge transfer of 0.199 e and a strong adsorption energy of −0.85 eV.[128] Banu et al. utilized M_2CO_2 MXene for the detection of NH_3 via oxygen functionalization.[129] Based on the detailed

DFT study, they reported the adsorption behaviour of NH_3 on Cr_2C/Fe_2C went through the alteration from chemisorption (E_{ad} = −1.40/−1.33 eV) to physisorption (E_{ad} = −0.29/−0.22 eV). Recently Quan et al. reported fully flexible $Ti_3C_2T_x$/WS_2 based gas sensor for NO_2 detection at room temperature.[130] To delve further into the sensing mechanism, adsorption models for NO_2 on $WS_2(001)$, $Ti_3C_2T_x(001)$, and $Ti_3C_2T_x(001)/WS_2(001)$ were computed using the DFT method. The calculated adsorption energies for NO_2 molecules on the surfaces of bare $WS_2(001)$, $Ti_3C_2T_x(001)$, and $Ti_3C_2T_x(001)/WS_2(001)$ were found to be −0.20 eV, −3.37 eV, and −3.73 eV, respectively. Weng et al. reported highly sensitive and selective $Ti_3C_2O_2$-based gas sensors for NH_3 sensing.[131] Through DFT study, they calculated adsorption energy of NH_3 on $Ti_3C_2O_2$ yields an appropriate value (−0.42 eV), and the charge transfer rate of 0.18 e. Based on their theoretical results, only NH_3 adsorbs onto the nanosheet through chemisorption. Reji et al. demonstrated the Sc_2CO_2 MXene nanosheets for detection of VOCs using first-principles DFT calculations.[132] They reported that 2-propanol (−0.63 eV), ethanol (−0.59 eV), and acetonitrile (−0.51 eV) show higher interaction with the Sc_2CO_2 MXene nanosheets. At the end, they also predict that Sc_2CO_2 MXene nanosheets can be utilized as a dual-mode sensor to detect potential VOC biomarkers in the exhaled breath.

8. Advantage and drawback of $Ti_3C_2T_x$ MXene gas sensors and other common materials

$Ti_3C_2T_x$ MXene is a promising material for gas sensors, but like any material, it has its advantages and drawbacks when

Table 1 Advantage and drawback of $Ti_3C_2T_x$ MXene with some common material

| S. no.	Materials	Advantages	Drawbacks
1.	$Ti_3C_2T_x$ MXene based gas senor	✓ High sensitivity ✓ Tunable properties ✓ Good conductivity ✓ Chemical stability	• Complex synthesis • Limited gas selectivity • Poor humidity sensitivity
2.	Metal oxide-based gas sensors (e.g., SnO_2 and ZnO)	✓ Low cost ✓ Commercial availability ✓ Good selectivity	• High operating temperature • Slow response/recovery • Limited sensitivity
3.	Organic polymer-based gas sensors	✓ Low cost ✓ Low power consumptions ✓ Tailorability	• Limited sensitivity • Limited durability • Limited operating range
	Other 2D materials (e.g., graphene, TMDs like MoS_2)		
4.	Graphene	✓ Excellent electrical conductivity ✓ Low noise levels ✓ High surface area	• Limited gas selectivity. • Difficulty in functionalizing for specific gas detection • Susceptibility to environmental factors, such as humidity
5.	TMDs	✓ Good gas selectivity due to varying band structures ✓ Layer-dependent properties for tenability ✓ Compatibility with existing semiconductor technologies.	• Moderate surface area compared to MXenes. • Synthesis challenges • Sensitivity to environmental conditions, including humidity.
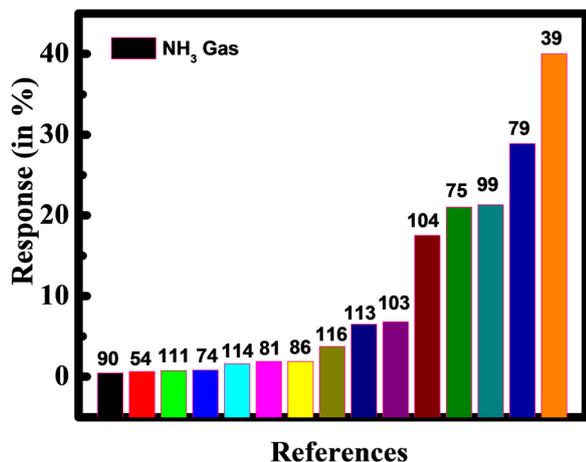
Fig. 11 Gas response of NH₃ gas with Ti₃C₂Tₓ MXene-based gas sensors.

compared to common materials used in gas sensing applications. The comparison of $Ti_3C_2T_x$ MXene with some common materials is given in Table 1.

In summary, $Ti_3C_2T_x$ MXene-based gas sensors offer unique advantages such as high surface area, tunability, and fast response times. However, they also face challenges related to synthesis complexity, moisture sensitivity, and limited gas range. The choice of gas sensor material depends on the specific application and requirements for sensitivity, selectivity, and operational conditions.

Our detailed study suggested that $Ti_3C_2T_x$ MXene-based gas sensors have a high response value for NH_3 gas. The response of NH_3 gas based on $Ti_3C_2T_x$ MXene with different literature has been shown in Fig. 11.

We have summarised the different types of $Ti_3C_2T_x$ MXene (pure, functionalized and compoite) based gas sensors in terms of sensitivity, limit of detection and working range in Table 2.

9. Conclusions and future prospective

MXenes are a newly discovered family of 2D materials that have been the subject of intensive research due to the exceptional properties that make them exceedingly valuable for use in various applications. MXene-based sensors have been among the most extensively researched applications because they are able to exploit the full potential of the one-of-a-kind 2D structure of MXenes. This is because MXenes have an inherently large specific surface area and surface-mediated properties that can be controlled. Thus, investigations on MXene-based gas sensors have been enhancing the selectivity and sensitivity using approaches such as composite formation, surface functionalization, and macro-structuring. The fact that the alternation of the MXene surface does not forfeit its fundamental outstanding electrical conductivity and improves its other physical and chemical properties makes it one of the most promising materials for sensors. For instance, it is conceivable to boost the adsorption energy of analytes on the

Table 2 Summary of $Ti_3C_2T_x$ MXene-based gas sensor

MXene	MXene type	Target gas	Sensitivity in %	Limit of detection (LOD)	Working range	Ref.
$Ti_3C_2T_x$	Pure	Ammonia	0.21	NR	25 to 200 ppm	75
	Pure	Acetone	0.97	0.011 ppb	50 ppb to 100 ppm	74
	Pure	Nitrogen dioxide	4.5	NR	5 ppm	91
	Pure	Ammonia	0.62	NR	5 ppm	54
	Pure	Ammonia	6.13	NR	10 to 700 ppm	86
	Pure	Ammonia	1.22	NR	1 to 100 ppm	133
	Pure	Methane	68	NR	200 to 10 000 ppm	134
	Pure	Toluene	19.32	NR	1 to 50 ppm	94
	Functionalized	Ethanol	9.99	NR	0.3 mM L^{-1} NaOH	93
	Functionalized	Hydrogen	23 ± 4	NR	0.5 to 40% H$_2$	96
	Functionalized	Toluene	79.5	NR	1 to 50 ppm	94
	Functionalized	Ammonia	28.87	NR	10 to 500 ppm	79
	Composite	Ethanol	14	NR	5 to 120 ppm	135
	Composite	Toluene	79.5	NR	1 to 50 ppm	94
	Composite	Hydrogen	70	NR	100 to 500 ppm	136
	Composite	Ammonia	6.2	NR	1 to 80 ppm	137
	Composite	Ammonia	3.1	NR	10 ppm	81
	Composite	Ammonia	0.4	NR	1 to 100 ppm	138
	Composite	Ammonia	24.8	NR	1 to 100 ppm	139
	Composite	Ammonia	22.3	NR	1 to 5 ppm	80
	Composite	Ammonia	40	4.29 ppb	0.5 to 100 ppm	39
	Composite	Ammonia	100.7	NR	20 ppm	140
	Composite	Toluene	11.4	NR	10 to 50 ppm	141
	Composite	Nitrogen dioxide	41.93	NR	5 to 100 ppm	142
	Composite	Nitrogen dioxide	37	125 ppb	0.125 to 5 ppm	101
	Composite	Nitrogen dioxide	165	50 ppb	0.05 to 20 ppm	143
	Composite	Acetone	0.25	0.05 ppm	0.05 to 30 ppm	144
	Composite	Acetone	52	NR	10 to 500 ppm	145
	Composite	Ethanol	27.4	NR	50 to 200 ppm	104
	Composite	Carbon dioxide	1	NR	8 to 3000 ppm	146
	Composite	Hexanal	3.4	217 ppb	10 to 40 ppm	147
	Composite	Methanol	29.6	NR	5 to 100 ppm	106

MXene surface while maintaining the material's conductivity. The aforementioned methods have proven to be successful in the majority of the research aimed at enhancing the performance of sensors.

The development of MXene-based sensors is still in its early stages; therefore, there are still issues that need to be resolved before they can be used commercially. There needs to be more information about these requirements because the performance standards and other requirements for putting these sensors on the market have not yet been developed in a systematic way. In this review, we have discussed the recent developments in the field of gas sensors based on 2D $Ti_3C_2T_x$ from three different perspectives: etching and delamination of $Ti_3C_2T_x$; pure, functional, and composite $Ti_3C_2T_x$ applied in gas sensors; and their sensing mechanism. The $Ti_3C_2T_x$ MXene has garnered a lot of attention and has been demonstrated to offer a lot of potential in the field of gas sensor. This is because of their one-of-a-kind structure and features. However, the application of $Ti_3C_2T_x$ in the real world is constrained by a number of different reasons. The first difficulty is associated with the process of preparing the MXene precursor, also known as the MAX phase. In most cases, the formation of a MAX phase occurs as a result of the high-temperature processing of combustible materials in powder forms, such as titanium, aluminum, and others. To obtain a MAX powder of the desired fineness, multiple milling processes are necessary. If HF is to be used as an etchant, the handling of HF and treatment of waste must be done correctly. The second obstacle is the mass production of MXene-based sensors, which is difficult because MXene does not have sufficient mechanical stability to be processed by industrial machines. In order to overcome this obstacle, researchers have been concentrating on the fabrication of nanocomposites by combining MXenes with a variety of other materials, particularly polymers. The third obstacle is determining the ideal proportion of MXene to incorporate into a polymer matrix in order to produce a high-performance sensor. The fourth obstacle pertains to applications that take place in the real world and require sensors to be durable and functional even after being damaged. This can be accomplished by modifying the surface of the components that make up a sensor, which in most cases results in improved mechanical properties of those components. The fifth obstacle is the requirement for clean and flawless MXene surfaces, which increases the sensitivity of MXene-based sensors. It is necessary to develop etchants that are superior to both HF and HCl/LiF. In general, the focus of research efforts on this subject at the moment is on exploring the maximal capability and potential of $Ti_3C_2T_x$ MXenes in terms of transferring their advantageous properties to sensors in order to obtain high performance of sensitivity and LOD. These aspects are absolutely necessary for the successful commercialization of MXene-based sensors. However, in order for MXenes to be successfully employed in the industry, several practical characteristics, including productivity, stability, and multifunctionality, should be examined and improved.

As a result, the area of future research should be broadened, and the primary objective should be to enhance sensor performance in terms of the variables described above so that it is compatible with industry requirements. In order to speed up the development of next-generation sensor technologies based on MXenes, it will be necessary to address the requirements listed above for commercialization. This will eventually pave the way for the creation of low-cost, high-performance, and multimodal sensors that can be used in soft-electronics applications. We hope this work will provide a roadmap for the commercialization of $Ti_3C_2T_x$ MXene-based gas sensors and encourage a wide range of in-depth and applicable studies in this area.

Conflicts of interest

All authors declare that they have no conflicts of interest. We certify that the submission is original work and is not under review at any other publication.

Acknowledgements

References

1 H. Zhang, L. Wang, Y. Zou, Y. Li, J. Xuan and X. Wang, et al., Enhanced ammonia sensing response based on Pt-decorated $Ti_3C_2T_x/TiO_2$ composite at room temperature, Nanotechnology, 2023, **34**, 205501.

2 Q. T. Lai, X. H. Zhao, Q. J. Sun, Z. Tang, X. G. Tang and V. A. Roy, Emerging MXene-Based Flexible Tactile Sensors for Health Monitoring and Haptic Perception, Small, 2023, 2300283.

3 R. Vishnuraj, M. Aleem, K. G. Nair and B. Pullithadathil, 1D aligned, n–p and n–n type ZnO heterojunction nanofibers for NO_2 sensors: exploration of conduction mechanism using in situ impedance spectroscopy, Mater. Adv., 2023, **4**, 3010–3025.

4 X. Kong, E. N. Tarakanova, X. Du, L. G. Tomilova and Y. Chen, Discrimination and detection of NO2, NH3 and H2S using sensor array based on three ambipolar sandwich tetradiazepinoporphyrazinato/phthalocyaninato europium double-decker complexes, Mater. Adv., 2023, **4**, 1515–1522.

5 H. Song, Y. Liu, Y. Fang and D. Zhang, Carbon-based electrochemical sensors for in vivo and in vitro neurotransmitter detection, Crit. Rev. Anal. Chem., 2023, **53**, 955–974.

6 F. M. Vivaldi, A. Dallinger, A. Bonini, N. Poma, L. Sembranti and D. Biagini, et al., Three-dimensional (3D) laser-induced graphene: structure, properties, and application to chemical sensing, ACS Appl. Mater. Interfaces, 2021, **13**, 30245–30260.

7 P. Qin, S. Okur, C. Li, A. Chandresh, D. Mutruc and S. Hecht, *et al.*, A photoprogrammable electronic nose with switchable selectivity for VOCs using MOF films, *Chem. Sci.*, 2021, **12**, 15700–15709.

8 H.-M. Yeung, G. Yoshikawa, K. Minami and K. Shiba, Strain-based chemical sensing using metal–organic framework nanoparticles, *J. Mater. Chem. A*, 2020, **8**, 18007–18014.

9 J. Chen, H. Lv, X. Bai, Z. Liu, L. He and J. Wang, *et al.*, Synthesis of hierarchically porous Co_3O_4/Biomass carbon composites derived from MOFs and their highly NO_2 gas sensing performance, *Microporous Mesoporous Mater.*, 2021, **321**, 111108.

10 X. Li, Y. Zhang, Y. Cheng, X. Chen and W. Tan, MOF-derived porous hierarchical $ZnCo_2O_4$ microflowers for enhanced performance gas sensor, *Ceram. Int.*, 2021, **47**, 9214–9224.

11 N. K. Chourasia, A. K. Singh, S. Rai, A. Sharma, P. Chakrabarti and A. Srivastava, *et al.*, A Lithography-Free Fabrication of Low-Operating Voltage-Driven, Very Large Channel Length Graphene Field-Effect Transistor With NH_3 Sensing Application, *IEEE Trans. Electron Devices*, 2020, **67**, 4385–4391.

12 N. K. Chourasia, V. K. Singh, A. Sharma, A. Srivastava and B. N. Pal, Lithography-free fabrication of low operating voltage and large channel length graphene transistor with current saturation by utilizing Li+ of ion-conducting-oxide gate dielectric, *AIP Adv.*, 2020, **10**, 085313.

13 G. Lei, C. Lou, X. Liu, J. Xie, Z. Li and W. Zheng, *et al.*, Thin films of tungsten oxide materials for advanced gas sensors, *Sens. Actuators, B*, 2021, **341**, 129996.

14 A. Sharma, N. K. Chourasia, A. Sugathan, Y. Kumar, S. Jit and S.-W. Liu, *et al.*, Solution processed Li_5AlO_4 dielectric for low voltage transistor fabrication and its application in metal oxide/quantum dot heterojunction phototransistors, *J. Mater. Chem. C*, 2018, **6**, 790–798.

15 N. K. Chourasia, A. Sharma, V. Acharya, N. Pal, S. Biring and B. N. Pal, Solution processed low band gap ion-conducting gate dielectric for low voltage metal oxide transistor, *J. Alloys Compd.*, 2019, **777**, 1124–1132.

16 N. Pal, A. Sharma, V. Acharya, N. K. Chourasia, S. Biring and B. N. Pal, Gate interface engineering for subvolt metal oxide transistor fabrication by using ion-conducting dielectric with Mn_2O_3 gate interface, *ACS Appl. Electron. Mater.*, 2019, **2**, 25–34.

17 A. Sharma, N. K. Chourasia, N. Pal, S. Biring and B. N. Pal, Role of electron donation of TiO_2 gate interface for developing solution-processed high-performance one-volt metal-oxide thin-film transistor using ion-conducting gate dielectric, *J. Phys. Chem. C*, 2019, **123**, 20278–20286.

18 V. Acharya, A. Sharma, N. K. Chourasia and B. N. Pal, Solution-processed $Pb_{0.8}Ba_{0.2}ZrO_3$ as a gate dielectric for low-voltage metal-oxide thin-film transistor, *Emergent Mater.*, 2020, **3**, 57–62.

19 N. K. Chourasia, A. Sharma, N. Pal, S. Biring and B. N. Pal, Dielectric/Semiconductor Interfacial p-Doping: A New Technique to Fabricate Solution-Processed High-Performance

1 V Ambipolar Oxide Transistors, *Phys. Status Solidi RRL*, 2020, **14**, 2000268.

20 A. Sharma, N. K. Chourasia, V. Acharya, N. Pal, S. Biring and S.-W. Liu, *et al.*, Ultra-low voltage metal oxide thin film transistor by low-temperature annealed solution processed $LiAlO_2$ gate dielectric, *Electron. Mater. Lett.*, 2020, **16**, 22–34.

21 A. K. Singh, N. K. Chourasia, B. N. Pal, A. Pandey and P. Chakrabarti, Low Operating Voltage Solution Processed (Li_2ZnO_2) Dielectric and (SnO_2) Channel-Based Medium Wave UV-B Phototransistor for Application in Phototherapy, *IEEE Trans. Electron Devices*, 2020, **67**, 2028–2034.

22 A. K. Singh, N. K. Chourasia, B. N. Pal, A. Pandey and P. Chakrabarti, A Proposed All ZnO Based Thin Film Transistor For UV-B Detection, *IEEE Photonics Technol. Lett.*, 2020, **32**, 1548–1551.

23 N. K. Chourasia and B. N. Pal, *Solution-processed photodetectors. Chemical Solution Synthesis for Materials Design and Thin Film Device Applications*, Elsevier, 2021, pp. 649–664.

24 U. Pandey, N. K. Chourasia, N. Pal, S. Biring and B. N. Pal, Functional Dielectric Properties of Solution-Processed Lithium Indium Tin Oxide ($LiInSnO_4$) and Its Application as a Gate Insulator of a Low Voltage Thin Film Transistor, *IEEE Trans. Electron Devices*, 2022, **69**, 1077–1082.

25 R. Saini, A. Mahajan, R. Bedi, D. Aswal and A. Debnath, Phthalocyanine based nanowires and nanoflowers as highly sensitive room temperature Cl_2 sensors, *RSC Adv.*, 2014, **4**, 15945–15951.

26 G. Chaloeipote, R. Prathumwan, K. Subannajui, A. Wisitsoraat and C. Wongchoosuk, 3D printed CuO semiconducting gas sensor for ammonia detection at room temperature, *Mater. Sci. Semicond. Process.*, 2021, **123**, 105546.

27 Y. Wang, S. Zhang, C. Huang, F. Qu, D. Yao and H. Guo, *et al.*, Mesoporous WO_3 modified by Au nanoparticles for enhanced trimethylamine gas sensing properties, *Dalton Trans.*, 2021, **50**, 970–978.

28 H. Sun, Y. Yao, R. Yang, Z. Yan, C. Cao and Y. Deng, *et al.*, A ZnO Gas Sensor with an Abnormal Response to Hydrogen, *Energies*, 2023, **16**, 5847.

29 S. Kumar, A. K. Sharma, M. K. Sohal, D. P. Sharma, A. Debnath and D. Aswal, *et al.*, Room temperature highly sensitive chlorine sensor based on reduced graphene oxide anchored with substituted copper phthalocyanine, *Sens. Actuators, B*, 2021, **327**, 128925.

30 M. Naguib, M. Kurtoglu, V. Presser, J. Lu, J. Niu and M. Heon, *et al.*, Two-dimensional nanocrystals produced by exfoliation of Ti_3AlC_2, *Adv. Mater.*, 2011, **23**, 4248–4253.

31 D. Dhamodharan, V. Dhinakaran and H.-S. Byun, MXenes: An emerging 2D material, *Carbon*, 2022, **192**, 366–383.

32 D. H. Ho, Y. Y. Choi, S. B. Jo, J. M. Myoung and J. H. Cho, Sensing with MXenes: progress and prospects, *Adv. Mater.*, 2021, **33**, 2005846.

33 Z. Ling, C. E. Ren, M.-Q. Zhao, J. Yang, J. M. Giammarco and J. Qiu, *et al.*, Flexible and conductive MXene films and nanocomposites with high capacitance, *Proc. Natl. Acad. Sci. U. S. A.*, 2014, **111**, 16676–16681.

34 H. Chen, Y. Wen, Y. Qi, Q. Zhao, L. Qu and C. Li, Pristine titanium carbide MXene films with environmentally stable conductivity and superior mechanical strength, *Adv. Funct. Mater.*, 2020, **30**, 1906996.

35 A. Rafieerad, W. Yan, G. L. Sequiera, N. Sareen, E. Abu-El-Rub and M. Moudgil, *et al.*, Application of Ti₃C₂ MXene quantum dots for immunomodulation and regenerative medicine, *Adv. Healthcare Mater.*, 2019, **8**, 1900569.

36 F. Shahzad, A. Iqbal, H. Kim and C. M. Koo, 2D transition metal carbides (MXenes): applications as an electrically conducting material, *Adv. Mater.*, 2020, **32**, 2002159.

37 Q. Yang, Y. Wang, X. Li, H. Li, Z. Wang and Z. Tang, *et al.*, Recent Progress of MX ene-Based Nanomaterials in Flexible Energy Storage and Electronic Devices, *Energy Environ. Mater.*, 2018, **1**, 183–195.

38 R. Zeng, W. Wang, M. Chen, Q. Wan, C. Wang and D. Knopp, *et al.*, CRISPR-Cas12a-driven MXene-PEDOT: PSS piezoresistive wireless biosensor, *Nano Energy*, 2021, **82**, 105711.

39 T. He, W. Liu, T. Lv, M. Ma, Z. Liu and A. Vasiliev, *et al.*, MXene/SnO₂ heterojunction based chemical gas sensors, *Sens. Actuators, B*, 2021, **329**, 129275.

40 L. Yang, H. Wang, W. Yuan, Y. Li, P. Gao and N. Tiwari, *et al.*, Wearable pressure sensors based on MXene/tissue papers for wireless human health monitoring, *ACS Appl. Mater. Interfaces*, 2021, **13**, 60531–60543.

41 Y. Chen, Y. Ge, W. Huang, Z. Li, L. Wu and H. Zhang, *et al.*, Refractive index sensors based on Ti₃C2Tₓ MXene fibers, *ACS Appl. Nano Mater.*, 2020, **3**, 303–311.

42 F. Guo, C. Feng, Z. Zhang, L. Zhang, C. Xu and C. Zhang, *et al.*, A room-temperature NO₂ sensor based on Ti₃C₂TX MXene modified with sphere-like CuO, *Sens. Actuators, B*, 2023, **375**, 132885.

43 X.-P. Li, Y. Li, X. Li, D. Song, P. Min and C. Hu, *et al.*, Highly sensitive, reliable and flexible piezoresistive pressure sensors featuring polyurethane sponge coated with MXene sheets, *J. Colloid Interface Sci.*, 2019, **542**, 54–62.

44 W. Hong, B. C. Wyatt, S. K. Nemani and B. Anasori, Double transition-metal MXenes: Atomistic design of two-dimensional carbides and nitrides, *MRS Bull.*, 2020, **45**, 850–861.

45 A. N. Kumar and K. Pal, Amine-functionalized stable Nb₂CTₓ MXene toward room temperature ultrasensitive NO₂ gas sensor, *Mater. Adv.*, 2022, **3**, 5151–5162.

46 G. Deysher, C. E. Shuck, K. Hantanasirisakul, N. C. Frey, A. C. Foucher and K. Maleski, *et al.*, Synthesis of Mo₄VAlC₄ MAX phase and two-dimensional Mo₄VC₄ MXene with five atomic layers of transition metals, *ACS Nano*, 2019, **14**, 204–217.

47 M. Alhabeb, K. Maleski, B. Anasori, P. Lelyukh, L. Clark and S. Sin, *et al.*, Guidelines for synthesis and processing of two-dimensional titanium carbide (Ti₃C₂Tₓ MXene), *Chem. Mater.*, 2017, **29**, 7633–7644.

48 W. Meng, X. Liu, H. Song, Y. Xie, X. Shi and M. Dargusch, *et al.*, Advances and challenges in 2D MXenes: From structures to energy storage and conversions, *Nano Today*, 2021, **40**, 101273.

49 M. Gupta, A. Verma, P. Chaudhary and B. Yadav, MXene and their integrated composite-based acetone sensors for monitoring of diabetes, *Mater. Adv.*, 2023, DOI: **10.1039/D3MA00188A**.

50 Y. Pei, X. Zhang, Z. Hui, J. Zhou, X. Huang and G. Sun, *et al.*, Ti₃C₂TX MXene for sensing applications: recent progress, design principles, and future perspectives, *ACS Nano*, 2021, **15**, 3996–4017.

51 Z. Sun, D. Music, R. Ahuja, S. Li and J. M. Schneider, Bonding and classification of nanolayered ternary carbides, *Phys. Rev. B: Condens. Matter Mater. Phys.*, 2004, **70**, 092102.

52 O. Mashtalir, M. Naguib, V. N. Mochalin, Y. Dall'Agnese, M. Heon and M. W. Barsoum, *et al.*, Intercalation and delamination of layered carbides and carbonitrides, *Nat. Commun.*, 2013, **4**, 1–7.

53 M. Li, J. Lu, K. Luo, Y. Li, K. Chang and K. Chen, *et al.*, Element replacement approach by reaction with Lewis acidic molten salts to synthesize nanolaminated MAX phases and MXenes, *J. Am. Chem. Soc.*, 2019, **141**, 4730–4737.

54 C. E. Shuck, M. Han, K. Maleski, K. Hantanasirisakul, S. J. Kim and J. Choi, *et al.*, Effect of Ti₃AlC₂ MAX phase on structure and properties of resultant Ti₃C₂Tₓ MXene, *ACS Appl. Nano Mater.*, 2019, **2**, 3368–3376.

55 J. Halim, M. R. Lukatskaya, K. M. Cook, J. Lu, C. R. Smith and L.-Å. Näslund, *et al.*, Transparent conductive two-dimensional titanium carbide epitaxial thin films, *Chem. Mater.*, 2014, **26**, 2374–2381.

56 M. Ghidiu, M. R. Lukatskaya, M.-Q. Zhao, Y. Gogotsi and M. W. Barsoum, Conductive two-dimensional titanium carbide 'clay' with high volumetric capacitance, *Nature*, 2014, **516**, 78–81.

57 A. Lipatov, M. Alhabeb, M. R. Lukatskaya, A. Boson, Y. Gogotsi and A. Sinitskii, Effect of synthesis on quality, electronic properties and environmental stability of individual monolayer Ti₃C₂ MXene flakes, *Adv. Electron. Mater.*, 2016, **2**, 1600255.

58 V.-H. Nguyen, B.-S. Nguyen, C. Hu, C. C. Nguyen, D. L. T. Nguyen and M. T. Nguyen Dinh, *et al.*, Novel architecture titanium carbide (Ti₃C₂Tₓ) MXene cocatalysts toward photocatalytic hydrogen production: a mini-review, *Nanomaterials*, 2020, **10**, 602.

59 J. Halim, J. Palisaitis, J. Lu, J. Thörnberg, E. Moon and M. Precner, *et al.*, Synthesis of two-dimensional Nb1. 33C (MXene) with randomly distributed vacancies by etching of the quaternary solid solution (Nb2/3Sc1/3) 2AlC MAX phase, *ACS Appl. Nano Mater.*, 2018, **1**, 2455–2460.

60 L. Wang, D. Liu, W. Lian, Q. Hu, X. Liu and A. Zhou, The preparation of V₂CTx by facile hydrothermal-assisted etching processing and its performance in lithium-ion battery, *J. Mater. Res. Technol.*, 2020, **9**, 984–993.

61 K. Maleski, V. N. Mochalin and Y. Gogotsi, Dispersions of two-dimensional titanium carbide MXene in organic solvents, *Chem. Mater.*, 2017, **29**, 1632–1640.

62 O. Mashtalir, M. R. Lukatskaya, A. I. Kolesnikov, E. Raymundo-Pinero, M. Naguib and M. Barsoum, *et al.*,

The effect of hydrazine intercalation on the structure and capacitance of 2D titanium carbide (MXene), *Nanoscale*, 2016, **8**, 9128–9133.

63 S. Yazdanparast, S. Soltanmohammad, A. Fash-White, G. J. Tucker and G. L. Brennecka, Synthesis and surface chemistry of 2D TiVC solid-solution MXenes, *ACS Appl. Mater. Interfaces*, 2020, **12**, 20129–20137.

64 H. L. Chia, C. C. Mayorga-Martinez, N. Antonatos, Z. K. Sofer, J. J. Gonzalez-Julian and R. D. Webster, *et al.*, MXene titanium carbide-based biosensor: strong dependence of exfoliation method on performance, *Anal. Chem.*, 2020, **92**, 2452–2459.

65 C. Xu, L. Wang, Z. Liu, L. Chen, J. Guo and N. Kang, *et al.*, Large-area high-quality 2D ultrathin Mo$_2$C superconducting crystals, *Nat. Mater.*, 2015, **14**, 1135–1141.

66 L. Verger, C. Xu, V. Natu, H.-M. Cheng, W. Ren and M. W. Barsoum, Overview of the synthesis of MXenes and other ultrathin 2D transition metal carbides and nitrides, *Curr. Opin. Solid State Mater. Sci.*, 2019, **23**, 149–163.

67 D. Wang, C. Zhou, A. S. Filatov, W. Cho, F. Lagunas and M. Wang, *et al.*, Direct synthesis and chemical vapor deposition of 2D carbide and nitride MXenes, *Science*, 2023, **379**, 1242–1247.

68 R. Qin, X. Li, M. Hu, G. Shan, R. Seeram and M. Yin, Preparation of high-performance MXene/PVA-based flexible pressure sensors with adjustable sensitivity and sensing range, *Sens. Actuators, A*, 2022, **338**, 113458.

69 X. Zeng, C. Zhao, X. Jiang, R. Yu and R. Che, Functional Tailoring of Multi-Dimensional Pure MXene Nanostructures for Significantly Accelerated Electromagnetic Wave Absorption, *Small*, 2023, 2303393.

70 R. Li, X. Ma, J. Li, J. Cao, H. Gao and T. Li, *et al.*, Flexible and high-performance electrochromic devices enabled by self-assembled 2D TiO$_2$/MXene heterostructures, *Nat. Commun.*, 2021, **12**, 1–11.

71 M. Naguib, O. Mashtalir, M. R. Lukatskaya, B. Dyatkin, C. Zhang and V. Presser, *et al.*, One-step synthesis of nanocrystalline transition metal oxides on thin sheets of disordered graphitic carbon by oxidation of MXenes, *Chem. Commun.*, 2014, **50**, 7420–7423.

72 X. Zhao, A. Vashisth, E. Prehn, W. Sun, S. A. Shah and T. Habib, *et al.*, Antioxidants unlock shelf-stable Ti$_3$C$_2$T$_x$ (MXene) nanosheet dispersions, *Matter*, 2019, **1**, 513–526.

73 M. Khazaei, M. Arai, T. Sasaki, C. Y. Chung, N. S. Venkataramanan and M. Estili, *et al.*, Novel electronic and magnetic properties of two-dimensional transition metal carbides and nitrides, *Adv. Funct. Mater.*, 2013, **23**, 2185–2192.

74 S. J. Kim, H.-J. Koh, C. E. Ren, O. Kwon, K. Maleski and S.-Y. Cho, *et al.*, Metallic Ti$_3$C$_2$T$_x$ MXene gas sensors with ultrahigh signal-to-noise ratio, *ACS Nano*, 2018, **12**, 986–993.

75 E. Lee, A. VahidMohammadi, B. C. Prorok, Y. S. Yoon, M. Beidaghi and D.-J. Kim, Room temperature gas sensing of two-dimensional titanium carbide (MXene), *ACS Appl. Mater. Interfaces*, 2017, **9**, 37184–37190.

76 W. Y. Chen, X. Jiang, S.-N. Lai, D. Peroulis and L. Stanciu, Nanohybrids of a MXene and transition metal dichalcogenide for selective detection of volatile organic compounds, *Nat. Commun.*, 2020, **11**, 1302.

77 B. Anasori, C. Shi, E. J. Moon, Y. Xie, C. A. Voigt and P. R. Kent, *et al.*, Control of electronic properties of 2D carbides (MXenes) by manipulating their transition metal layers, *Nanoscale Horiz.*, 2016, **1**, 227–234.

78 Y. Zhang, Y. Jiang, Z. Duan, Q. Huang, Y. Wu and B. Liu, *et al.*, Highly sensitive and selective NO$_2$ sensor of alkalized V$_2$CTx MXene driven by interlayer swelling, *Sens. Actuators, B*, 2021, **344**, 130150.

79 Z. Yang, A. Liu, C. Wang, F. Liu, J. He and S. Li, *et al.*, Improvement of gas and humidity sensing properties of organ-like MXene by alkaline treatment, *ACS Sens.*, 2019, **4**, 1261–1269.

80 X. Guo, Y. Ding, D. Kuang, Z. Wu, X. Sun and B. Du, *et al.*, Enhanced ammonia sensing performance based on MXene-Ti$_3$C$_2$T$_x$ multilayer nanoflakes functionalized by tungsten trioxide nanoparticles, *J. Colloid Interface Sci.*, 2021, **595**, 6–14.

81 H. Tai, Z. Duan, Z. He, X. Li, J. Xu and B. Liu, *et al.*, Enhanced ammonia response of Ti$_3$C$_2$T$_x$ nanosheets supported by TiO$_2$ nanoparticles at room temperature, *Sens. Actuators, B*, 2019, **298**, 126874.

82 D. Zhang, S. Yu, X. Wang, J. Huang, W. Pan and J. Zhang, *et al.*, UV illumination-enhanced ultrasensitive ammonia gas sensor based on (001) TiO$_2$/MXene heterostructure for food spoilage detection, *J. Hazard. Mater.*, 2022, **423**, 127160.

83 P. K. Kalambate, N. S. Gadhari, X. Li, Z. Rao, S. T. Navale and Y. Shen, *et al.*, Recent advances in MXene–based electrochemical sensors and biosensors, *TrAC, Trends Anal. Chem.*, 2019, **120**, 115643.

84 J. Ran, G. Gao, F.-T. Li, T.-Y. Ma, A. Du and S.-Z. Qiao, Ti$_3$C$_2$ MXene co-catalyst on metal sulfide photo-absorbers for enhanced visible-light photocatalytic hydrogen production, *Nat. Commun.*, 2017, **8**, 1–10.

85 H. Liao, X. Guo, P. Wan and G. Yu, Conductive MXene nanocomposite organohydrogel for flexible, healable, low-temperature tolerant strain sensors, *Adv. Funct. Mater.*, 2019, **29**, 1904507.

86 M. Wu, M. He, Q. Hu, Q. Wu, G. Sun and L. Xie, *et al.*, Ti$_3$C$_2$ MXene-based sensors with high selectivity for NH$_3$ detection at room temperature, *ACS Sens.*, 2019, **4**, 2763–2770.

87 P. Khakbaz, M. Moshayedi, S. Hajian, M. Soleimani, B. B. Narakathu and B. J. Bazuin, *et al.*, Titanium carbide MXene as NH$_3$ sensor: realistic first-principles study, *J. Phys. Chem. C*, 2019, **123**, 29794–29803.

88 F. Zeng, X. Feng, X. Chen, Q. Yao, Y. Miao and L. Dai, *et al.*, First-principles analysis of Ti$_3$C$_2$T$_x$ MXene as a promising candidate for SF$_6$ decomposition characteristic components sensor, *Appl. Surf. Sci.*, 2022, **578**, 152020.

89 S. Huang and V. N. Mochalin, Understanding chemistry of two-dimensional transition metal carbides and carbonitrides (MXenes) with gas analysis, *ACS Nano*, 2020, **14**, 10251–10257.

90 S. J. Kim, J. Choi, K. Maleski, K. Hantanasirisakul, H.-T. Jung and Y. Gogotsi, et al., Interfacial assembly of ultrathin, functional MXene films, ACS Appl. Mater. Interfaces, 2019, 11, 32320–32327.

91 Y. Chae, S. J. Kim, S.-Y. Cho, J. Choi, K. Maleski and B.-J. Lee, et al., An investigation into the factors governing the oxidation of two-dimensional Ti$_3$C$_2$ MXene, Nanoscale, 2019, 11, 8387–8393.

92 X. Li, Z. An, Y. Lu, J. Shan, H. Xing and G. Liu, et al., Room Temperature VOCs Sensing with Termination-Modified Ti$_3$C$_2$T$_x$ MXene for Wearable Exhaled Breath Monitoring, Adv. Mater. Technol., 2022, 7, 2100872.

93 H.-J. Koh, S. J. Kim, K. Maleski, S.-Y. Cho, Y.-J. Kim and C. W. Ahn, et al., Enhanced selectivity of MXene gas sensors through metal ion intercalation: in situ X-ray diffraction study, ACS Sens., 2019, 4, 1365–1372.

94 S. N. Shuvo, A. M. Ulloa Gomez, A. Mishra, W. Y. Chen, A. M. Dongare and L. A. Stanciu, Sulfur-doped titanium carbide MXenes for room-temperature gas sensing, ACS Sens., 2020, 5, 2915–2924.

95 H. Pazniak, I. A. Plugin, M. J. Loes, T. M. Inerbaev, I. N. Burmistrov and M. Gorshenkov, et al., Partially Oxidized Ti$_3$C$_2$T$_x$ MXenes for Fast and Selective Detection of Organic Vapors at Part-per-Million Concentrations, ACS Appl. Nano Mater., 2020, 3, 3195–3204.

96 Z. Zhu, C. Liu, F. Jiang, J. Liu, X. Ma and P. Liu, et al., Flexible and lightweight Ti$_3$C$_2$T$_x$ MXene@ Pd colloidal nanoclusters paper film as novel H$_2$ sensor, J. Hazard. Mater., 2020, 399, 123054.

97 E. S. Muckley, M. Naguib, H.-W. Wang, L. Vlcek, N. C. Osti and R. L. Sacci, et al., Multimodality of structural, electrical, and gravimetric responses of intercalated MXenes to water, ACS Nano, 2017, 11, 11118–11126.

98 N. Shpigel, M. D. Levi, S. Sigalov, T. S. Mathis, Y. Gogotsi and D. Aurbach, Direct assessment of nanoconfined water in 2D Ti$_3$C$_2$ electrode interspaces by a surface acoustic technique, J. Am. Chem. Soc., 2018, 140, 8910–8917.

99 L. Yao, X. Tian, X. Cui, R. Zhao, X. Xiao and Y. Wang, Partially oxidized Ti$_3$C$_2$T$_x$ MXene-sensitive material-based ammonia gas sensor with high-sensing performances for room temperature application, J. Mater. Sci.: Mater. Electron., 2021, 32, 27837–27848.

100 L. Lorencova, T. Bertok, J. Filip, M. Jerigova, D. Velic and P. Kasak, et al., Highly stable Ti$_3$C$_2$T$_x$ (MXene)/Pt nanoparticles-modified glassy carbon electrode for H$_2$O$_2$ and small molecules sensing applications, Sens. Actuators, B, 2018, 263, 360–368.

101 J. Choi, Y. J. Kim, S. Y. Cho, K. Park, H. Kang and S. J. Kim, et al., In situ formation of multiple Schottky barriers in a Ti$_3$C$_2$ MXene film and its application in highly sensitive gas sensors, Adv. Funct. Mater., 2020, 30, 2003998.

102 W. Y. Chen, X. Jiang, S.-N. Lai, D. Peroulis and L. Stanciu, Nanohybrids of a MXene and transition metal dichalcogenide for selective detection of volatile organic compounds, Nat. Commun., 2020, 11, 1–10.

103 S. H. Lee, W. Eom, H. Shin, R. B. Ambade, J. H. Bang, H. W. Kim, et al., Room-Temperature, Highly Durable Ti$_3$C$_2$T$_x$ MXene/Graphene Hybrid Fibers for NH$_3$ Gas Sensing, 2020.

104 L. Zhao, K. Wang, W. Wei, L. Wang and W. Han, High-performance flexible sensing devices based on polyaniline/MXene nanocomposites, InfoMat, 2019, 1, 407–416.

105 S. Sun, M. Wang, X. Chang, Y. Jiang, D. Zhang and D. Wang, et al., W18O49/Ti$_3$C$_2$T$_x$ Mxene nanocomposites for highly sensitive acetone gas sensor with low detection limit, Sens. Actuators, B, 2020, 304, 127274.

106 M. Liu, Z. Wang, P. Song, Z. Yang and Q. Wang, In$_2$O$_3$ nanocubes/Ti$_3$C$_2$T$_x$ MXene composites for enhanced methanol gas sensing properties at room temperature, Ceram. Int., 2021, 47, 23028–23037.

107 Y. Xia, S. He, J. Wang, L. Zhou, J. Wang and S. Komarneni, MXene/WS$_2$ hybrids for visible-light-activated NO$_2$ sensing at room temperature, Chem. Commun., 2021, 57, 9136–9139.

108 A. K. Pandey, Graphene–Ti$_3$C$_2$T$_x$ MXene hybrid nanostructure: a promising material for sensitivity enhancement in plasmonic sensor, Appl. Phys. A: Mater. Sci. Process., 2021, 127, 1–6.

109 Z.-D. Hu, X.-Y. Sun, H.-F. Li, Y.-R. Kang, X.-Q. Song and P. Wang, et al., Cobalt monosulfide nanofibers: ethanol sensing and magnetic properties, Rare Met., 2021, 40, 1554–1560.

110 H. Yan, L. Chu, Z. Li, C. Sun, Y. Shi and J. Ma, 2H-MoS$_2$/Ti$_3$C$_2$T$_x$ MXene composites for enhanced NO$_2$ gas sensing properties at room temperature, Sens. Actuators Rep., 2022, 4, 100103.

111 W. Yuan, K. Yang, H. Peng, F. Li and F. Yin, A flexible VOCs sensor based on a 3D Mxene framework with a high sensing performance, J. Mater. Chem. A, 2018, 6, 18116–18124.

112 S. H. Lee, W. Eom, H. Shin, R. B. Ambade, J. H. Bang and H. W. Kim, et al., Room-temperature, highly durable Ti$_3$C$_2$T$_x$ MXene/graphene hybrid fibers for NH$_3$ gas sensing, ACS Appl. Mater. Interfaces, 2020, 12, 10434–10442.

113 Z. Yang, H. Zou, Y. Zhang, F. Liu, J. Wang and S. Lv, et al., The Introduction of Defects in Ti$_3$C$_2$T$_x$ and Ti$_3$C$_2$T$_x$-Assisted Reduction of Graphene Oxide for Highly Selective Detection of ppb-Level NO$_2$, Adv. Funct. Mater., 2022, 32, 2108959.

114 X. Li, J. Xu, Y. Jiang, Z. He, B. Liu and H. Xie, et al., Toward agricultural ammonia volatilization monitoring: A flexible polyaniline/Ti$_3$C$_2$T$_x$ hybrid sensitive films based gas sensor, Sens. Actuators, B, 2020, 316, 128144.

115 X. Wang, K. Sun, K. Li, X. Li and Y. Gogotsi, Ti$_3$C$_2$T$_x$/PEDOT: PSS hybrid materials for room-temperature methanol sensor, Chin. Chem. Lett., 2020, 31, 1018–1021.

116 P. Chen, Z. Zhao, Z. Shao, Y. Tian, B. Li and B. Huang, et al., Highly selective NH$_3$ gas sensor based on polypyrrole/Ti$_3$C$_2$T$_x$ nanocomposites operating at room temperature, J. Mater. Sci.: Mater. Electron., 2022, 33, 6168–6177.

117 S. Sardana, Z. Singh, A. K. Sharma, N. Kaur, P. K. Pati and A. Mahajan, Self-powered biocompatible humidity sensor

based on an electrospun anisotropic triboelectric nanogenerator for non-invasive diagnostic applications, *Sens. Actuators, B*, 2022, **371**, 132507.

118 S. Sardana, H. Kaur, B. Arora, D. K. Aswal and A. Mahajan, Self-powered monitoring of ammonia using an MXene/TiO₂/cellulose nanofiber heterojunction-based sensor driven by an electrospun triboelectric nanogenerator, *ACS Sens.*, 2022, **7**, 312–321.

119 M. Wang, W. Liu, X. Shi, Y. Cong, S. Lin and T. Sun, *et al.*, Self-powered and low-temperature resistant MXene-modified electronic-skin for multifunctional sensing, *Chem. Commun.*, 2021, **57**, 8790–8793.

120 S. Gasso and A. Mahajan, Self-Powered Wearable Gas Sensors Based on l-Ascorbate-Treated MXene Nanosheets and SnO₂ Nanofibers, *ACS Appl. Nano Mater.*, 2023, **6**, 6678–6692.

121 D. Wang, D. Zhang, J. Guo, Y. Hu, Y. Yang and T. Sun, *et al.*, Multifunctional poly(vinyl alcohol)/Ag nanofibers-based triboelectric nanogenerator for self-powered MXene/tungsten oxide nanohybrid NO₂ gas sensor, *Nano Energy*, 2021, **89**, 106410.

122 X.-F. Yu, Y.-C. Li, J.-B. Cheng, Z.-B. Liu, Q.-Z. Li and W.-Z. Li, *et al.*, Monolayer Ti₂CO₂: a promising candidate for NH₃ sensor or capturer with high sensitivity and selectivity, *ACS Appl. Mater. Interfaces*, 2015, **7**, 13707–13713.

123 B. Xiao, Y.-C. Li, X.-F. Yu and J.-B. Cheng, MXenes: Reusable materials for NH₃ sensor or capturer by controlling the charge injection, *Sens. Actuators, B*, 2016, **235**, 103–109.

124 Y. Wang, S. Ma, L. Wang and Z. Jiao, A novel highly selective and sensitive NH₃ gas sensor based on monolayer Hf₂CO₂, *Appl. Surf. Sci.*, 2019, **492**, 116–124.

125 S. Hajian, P. Khakbaz, M. Moshayedi, D. Maddipatla, B. B. Narakathu, V. S. Turkani, *et al.* Impact of different ratios of fluorine, oxygen, and hydroxyl surface terminations on Ti₃C₂Tₓ MXene as ammonia sensor: a first-principles study, *2018 IEEE SENSORS*: IEEE, 2018, pp. 1–4.

126 Y. Zhang, Z. Zhou, J. Lan and P. Zhang, Prediction of Ti₃C₂O₂ MXene as an effective capturer of formaldehyde, *Appl. Surf. Sci.*, 2019, **469**, 770–774.

127 S. Ma, D. Yuan, Z. Jiao, T. Wang and X. Dai, Monolayer Sc₂CO₂: a promising candidate as a SO₂ gas sensor or capturer, *J. Phys. Chem. C*, 2017, **121**, 24077–24084.

128 D. Yang, X. Fan, D. Zhao, Y. An, Y. Hu and Z. Luo, Sc₂CO₂ and Mn-doped Sc₂CO₂ as gas sensor materials to NO and CO: A first-principles study, *Phys. E*, 2019, **111**, 84–90.

129 A. A. Banu, S. Sinthika, S. Premkumar, J. Vigneshwaran, S. Z. Karazhanov and S. P. Jose, DFT study of NH₃ adsorption on 2D monolayer MXenes (M₂C, M= Cr, Fe) via oxygen functionalization: Suitable materials for gas sensors, *FlatChem*, 2022, **31**, 100329.

130 W. Quan, J. Shi, H. Luo, C. Fan, W. Lv and X. Chen, *et al.*, Fully Flexible MXene-based Gas Sensor on Paper for Highly Sensitive Room-Temperature Nitrogen Dioxide Detection, *ACS Sens.*, 2023, **8**, 103–113.

131 K. Weng, J. Peng, Z. Shi, A. Arramel and N. Li, Highly NH₃ Sensitive and Selective Ti₃C₂O₂-Based Gas Sensors: A Density Functional Theory-NEGF Study, *ACS Omega*, 2023, **8**, 4261–4269.

132 R. P. Reji, S. K. C. Balaji, Y. Sivalingam, Y. Kawazoe and S. Velappa Jayaraman, First-Principles Density Functional Theory Calculations on the Potential of Sc₂CO₂ MXene Nanosheets as a Dual-Mode Sensor for Detection of Volatile Organic Compounds in Exhaled Human Breath, *ACS Appl. Nano Mater.*, 2023, **6**, 5345–5356.

133 Y. Jian, D. Qu, L. Guo, Y. Zhu, C. Su and H. Feng, *et al.*, The prior rules of designing Ti₃C₂Tₓ MXene-based gas sensors, *Front. Chem. Sci. Eng.*, 2021, **15**, 505–517.

134 J. Wang, R. Xu, Y. Xia and S. Komarneni, Ti₂CTx MXene: A novel p-type sensing material for visible light-enhanced room temperature methane detection, *Ceram. Int.*, 2021, **47**, 34437–34442.

135 W. Y. Chen, S.-N. Lai, C.-C. Yen, X. Jiang, D. Peroulis and L. A. Stanciu, Surface functionalization of Ti₃C₂Tₓ MXene with highly reliable superhydrophobic protection for volatile organic compounds sensing, *ACS Nano*, 2020, **14**, 11490–11501.

136 S. A. M. Chachuli, M. N. Hamidon, M. Ertugrul, M. S. Mamat, O. Coban and F. N. Tuzluca, *et al.*, Effects of MWCNTs/graphene nanoflakes/MXene addition to TiO₂ thick film on hydrogen gas sensing, *J. Alloys Compd.*, 2021, **882**, 160671.

137 D. Kuang, X. Guo, Z. Zhu, Y. Ding, X. Sun and Z. Wu, *et al.*, Enhanced room temperature ammonia response of 2D-Ti₃C₂Tₓ MXene decorated with Ni (OH)₂ nanoparticles, *Ceram. Int.*, 2021, **47**, 19471–19480.

138 Q. Sun, J. Wang, X. Wang, J. Dai, X. Wang and H. Fan, *et al.*, Treatment-dependent surface chemistry and gas sensing behavior of the thinnest member of titanium carbide MXenes, *Nanoscale*, 2020, **12**, 16987–16994.

139 D. Wang, D. Zhang, Y. Yang, Q. Mi, J. Zhang and L. Yu, Multifunctional latex/polytetrafluoroethylene-based triboelectric nanogenerator for self-powered organ-like MXene/metal–organic framework-derived CuO nanohybrid ammonia sensor, *ACS Nano*, 2021, **15**, 2911–2919.

140 Z. Liu, T. He, H. Sun, B. Huang and X. Li, Layered MXene heterostructured with In₂O₃ nanoparticles for ammonia sensors at room temperature, *Sens. Actuators, B*, 2022, **365**, 131918.

141 A. Hermawan, B. Zhang, A. Taufik, Y. Asakura, T. Hasegawa and J. Zhu, *et al.*, CuO Nanoparticles/Ti₃C₂Tₓ MXene Hybrid Nanocomposites for Detection of Toluene Gas, *ACS Appl. Nano Mater.*, 2020, **3**, 4755–4766.

142 Z. Yang, L. Jiang, J. Wang, F. Liu, J. He and A. Liu, *et al.*, Flexible resistive NO₂ gas sensor of three-dimensional crumpled MXene Ti₃C₂Tₓ/ZnO spheres for room temperature application, *Sens. Actuators, B*, 2021, **326**, 128828.

143 Y. Song, Y. Xu, Q. Guo, Z. Hua, F. Yin and W. Yuan, MXene-derived TiO₂ nanoparticles intercalating between RGO nanosheets: an assembly for highly sensitive gas detection, *ACS Appl. Mater. Interfaces*, 2021, **13**, 39772–39780.

144 Y. Tang, Y. Xu, J. Yang, Y. Song, F. Yin and W. Yuan, Stretchable and wearable conductometric VOC sensors

based on microstructured MXene/polyurethane core-sheath fibers, *Sens. Actuators, B*, 2021, **346**, 130500.

145 M. Liu, Z. Wang, P. Song, Z. Yang and Q. Wang, Flexible MXene/rGO/CuO hybrid aerogels for high performance acetone sensing at room temperature, *Sens. Actuators, B*, 2021, **340**, 129946.

146 Y. Zhou, Y. Wang, Y. Wang and X. Li, Humidity-Enabled Ionic Conductive Trace Carbon Dioxide Sensing of Nitrogen-Doped $Ti_3C_2T_x$ MXene/Polyethyleneimine Composite Films Decorated with Reduced Graphene Oxide Nanosheets, *Anal. Chem.*, 2020, **92**, 16033–16042.

147 D. Kuang, L. Wang, X. Guo, Y. She, B. Du and C. Liang, *et al.*, Facile hydrothermal synthesis of $Ti_3C_2T_x$-TiO_2 nanocomposites for gaseous volatile organic compounds detection at room temperature, *J. Hazard. Mater.*, 2021, **416**, 126171.